39p

[redacted]

461

Copy
RM E57A07

RESEARCH MEMORANDUM

INVESTIGATION OF AN AIR-COOLED, PLUG-TYPE, VARIABLE-AREA EXHAUST NOZZLE

By G. R. Smolak and W. K. Koffel

Lewis Flight Propulsion Laboratory
Cleveland, Ohio

CLASSIFIED DOCUMENT

This material contains information affecting the National Defense of the United States within the meaning of the espionage laws, Title 18, U.S.C., Secs. 793 and 794, the transmission or revelation of which in any manner to an unauthorized person is prohibited by law.

NATIONAL ADVISORY COMMITTEE
FOR AERONAUTICS

WASHINGTON

April 10, 1957

[redacted]

NACA RM E57A07

NATIONAL ADVISORY COMMITTEE FOR AERONAUTICS

RESEARCH MEMORANDUM

INVESTIGATION OF AN AIR-COOLED, PLUG-TYPE, VARIABLE-AREA EXHAUST NOZZLE

By G. R. Smolak and W. K. Koffel

SUMMARY

The cooling requirements and internal thrust performance of an air-cooled, plug-type, variable-area exhaust nozzle were experimentally investigated in a turbojet-engine afterburner over a range of exhaust-gas total temperatures from 1990° to 2840° F and a range of exhaust-nozzle pressure ratios from 1.5 to 10.8.

At the highest exhaust-gas total temperature investigated (2840° F), a total nozzle cooling airflow of 4.5 percent of the afterburner gas flow produced an average plug surface temperature of 1620° F. The 4.5 percent value comprised about 1.2 percent for plug cooling, 2.6 percent for plug support-strut cooling, and 0.7 percent for outer-shell cooling.

The value of the jet-thrust coefficient was constant at about 0.97 over a range of exhaust-nozzle pressure ratios from 1.5 to 10.8 for the full-scale plug nozzle with a smooth fairing on the tailcone. This level of internal thrust performance was good and agreed well with prior NACA model-plug-nozzle data. A loss in jet-thrust coefficient up to 2 percent was caused by roughness (discontinuities and buckles) on the plug tailcone surface.

INTRODUCTION

The plug-type nozzle appears promising for application to current supersonic aircraft. Model studies of plug-type nozzles (refs. 1 to 5) have shown that internal-thrust performance is good at both low and high nozzle pressure ratios. Thus, both subsonic and supersonic levels of internal-thrust coefficient are high.

Cooling problems arise from the presence of the plug in the high-temperature exhaust gas. Both the amount of cooling required and any undesirable effect of the cooling system on the internal-thrust performance of the nozzle are important considerations.

In order to obtain information on plug-nozzle cooling problems and internal-thrust performance, a full-scale, air-cooled, variable-area plug nozzle was built and run at the NACA Lewis laboratory. The conical plug nozzle was installed on a turbojet-engine afterburner. Cooling requirements of the nozzle at high exhaust-gas temperatures and pressures were evaluated in a sea-level exhaust facility where control of engine-inlet ram ratio was available. The internal-thrust performance of the nozzle was evaluated in an altitude exhaust facility that provided a broad range of exhaust-nozzle pressure ratios.

A wide range of conditions was covered in these tests. The exhaust-gas total temperature was varied from 1990° to 2840° F. The total cooling airflow was varied from 0.7 to 4.5 percent of the afterburner gas flow. The exhaust-nozzle pressure ratio was varied from 1.5 to 10.8.

APPARATUS

Exhaust Nozzle

Description of conical plug. - The complete, air-cooled, plug-type, variable-area exhaust nozzle installed in an afterburner is shown in figure 1. The nose of the plug was spherical and faired into a conical tail. Three struts supported the plug and held the cooling-air and instrumentation ducts. For experimental convenience, the nozzle was designed so that throat-area variation could be effected by axial translation of the plug.

The plug envelope dimensions are specified in figure 2. The maximum diameter of the plug was 20 inches and its over-all length was 31.40 inches. For one part of the internal-thrust investigation, a smooth fairing was put on the plug tailcone, as shown in figure 3.

Plug cooling systems. - The cooling systems chosen for the plug employed both forced convection and film cooling. Details of the cooling systems are shown in figures 1 and 4. Plug cooling air flowed through the traverse tubes, the struts, and the tubes inside the plug and finally discharged through nine annular slots on the plug surface. Folded wire screen in the slots served to meter the flow of air from the slots. The double-walled nose cap was cooled by forced convection. The region around a typical slot in the tailcone was cooled by (1) the internal forced convection on the under side of the surface by air flowing through the manifold and slot, (2) the conduction to adjacent blowing slot manifolds acting as heat sinks, and (3) the film of air blowing from the slot.

Strut cooling system. - Strut cooling air first flowed through the center passages of the traverse tubes and the struts to the plug interior. It then passed out through the annular passage beneath each strut outer

jacket and into the main gas stream at the outer end of each strut. Cooling of the strut jackets was augmented by fins on the inner jacket surface and by conduction to the plug cooling-air supply ducts inside of each strut. The strut cooling air, while inside of the plug, caused additional forced-convection cooling of the inner plug surfaces.

Outer-shell cooling systems. - Two outer shells were employed (see fig. 5) in this cooling system. One outer shell employed the forced-convection film-cooling arrangement used for the plug. The other was cooled by extending the corrugated louvered liner of the combustion chamber to the nozzle lip.

The forced-convection film-cooled outer shell is shown in detail in figure 6(a). The lip angle was 51.5° measured with reference to the centerline of the engine, and the lip diameter was 26.88 inches. The shell surface was cooled by air flowing through the manifolds and through the screen in the slot.

The important features of the outer shell cooled with a corrugated louvered liner are shown in figure 6(b). The lip angle of this outer shell was 39.63°, and the lip diameter was 24.74 inches. Cooling for the conical shell was provided by extending the combustion-chamber liner to the nozzle lip, thus utilizing the relatively cool gas between the liner and the wall.

Engine and Afterburner

A production turbojet engine was used as a gas generator for this investigation. The engine-inlet airflow was 102 pounds per second at the rated speed of 7950 rpm. An afterburner of NACA design was fitted to the engine. The principal afterburner details are shown in figure 7. Fuel-spray-bar details are shown in figure 8. Thirty-eight fuel spray bars were arranged in two rows of 19 bars each with an axial spacing of 3.08 inches between the rows. The upstream row was 31.51 inches upstream of the trailing edge of the flameholder. A two-ring, annular, V-gutter flameholder was used. Cooling of the afterburner wall was provided by a corrugated louvered liner (fig. 9) extending from the flameholder to the exhaust-nozzle inlet. The liner inhibited screech and cooled the afterburner wall.

Facilities

The two phases of the investigation, cooling and internal thrust, were conducted in different facilities. For the cooling phase of the investigation, the nozzle and engine were installed in a sea-level exhaust facility. The exhaust gases were discharged into an acoustical muffler at atmospheric pressure. For the internal-thrust phase of the investigation, the engine and nozzle were installed in an altitude exhaust facility.

Instrumentation

Engine. - The instrumentation used in the engine and afterburner is shown in figure 7. At the engine inlet (station 1), airflow surveys of total pressure, static pressure, and total temperature were made. Surveys of total pressure and total temperature were made at the turbine discharge (station 2). A total-pressure survey was made at station 3, just ahead of the plug nozzle.

Outer shells. - The exhaust-nozzle instrumentation consisted of thermocouples and pressure taps on the outer shell, the plug, and in the cooling-air passages. On the convection-cooled outer shell, temperature measurements were made at several locations on the gas side of the inner surface (fig. 6(a)). Cooling airflow to this outer shell was measured in a separate supply pipe. Measurements were also made of the pressure inside the manifold supplying cooling air to the outer shell. Instrumentation on the liner-cooled outer shell consisted of temperature measurements at several locations on the gas side of the inner surface, as shown in figure 6(b).

Plug. - Details of the plug instrumentation are shown in figures 1, 10, and 11. A complete longitudinal survey was made of static pressure on the plug surface. Plug surface temperatures were measured in three circumferential positions downstream of each cooling-air slot. Strut jacket temperature was measured with a single thermocouple on the leading edge of each strut. Static pressure was measured in each manifold supplying the slots and in the plug interior. The cooling airflow to each slot was measured with an individual supply pipe. Each pipe was instrumented with a thermocouple and static- and total-pressure taps.

Thermocouple construction. - All thermocouples used in the plug, the struts, and the outer shell were of the swaged type, thus providing ease of installation and durability. The chromel-alumel wires were surrounded by magnesium-oxide insulation and were contained in a seamless Inconel tube. The entire assembly was then drawn through a die, crushing the insulation. Welding of the swaged-type thermocouple to a metal skin provided a fin action for dissipation of heat to cold air blowing over the thermocouple lead. This effect caused an appreciable local depression of the surface temperature at the thermocouple junction compared with the surface temperature in the absence of the thermocouple. A correction was applied to the thermocouple reading to compensate for this effect (see appendix B).

Scale-force and fuel-flow measurements. - Scale force was measured with a self-balancing null-type pneumatic thrust cell. Fuel flow was measured with calibrated vane-type flowmeters. The types of fuel used during the cooling and thrust performance investigations were MIL-F-5624C, grade JP-5, and MIL-F-5624C, grade JP-4, respectively.

PROCEDURE

Cooling-Requirements Investigation

Investigation of the cooling requirements of the exhaust nozzle was conducted in a sea-level exhaust facility. At a constant level of exhaust-gas total temperature, the plug, strut, and outer-shell cooling airflows were varied over a range of values in order to produce safe strut and outer-shell temperatures and predetermined levels of average plug surface temperature. This procedure was repeated at several different exhaust-gas total temperatures between 1990° and 2840° F. Cooling air was independently supplied from laboratory compressors.

Internal-Thrust Investigation

The investigation of the internal-thrust performance of the plug nozzle was conducted under nonafterburning conditions in an altitude exhaust facility. The primary variables were exhaust-nozzle operating pressure ratio, nozzle-area ratio, and geometry of the outer shell. Internal-thrust performance of each configuration was measured over a range of exhaust-nozzle pressure ratios. Exhaust-nozzle pressure ratio was adjusted by changing the exhaust-gas total pressure and/or the simulated altitude pressure to which the engine exhausted. Nozzle-area ratio was adjusted by longitudinal translation of the plug parallel to the centerline of the engine. The range of area ratio available was from 1.11 to 1.85. Cooling airflow to the slots and struts was varied from zero to maximum flow in various combinations to determine the effect of individual coolant flows on internal thrust.

Computations

Appendix A contains a list of all the symbols used in this report. Appendix B specifies the methods used to compute cooling airflows, exhaust-nozzle gas flow, jet-thrust coefficient, exhaust-gas total temperature, and swaged-thermocouple corrections.

RESULTS AND DISCUSSION

Cooling Performance

The plug surface, the support struts, and the outer shells required separate cooling systems. The plug itself was the major item of interest in this cooling investigation, because it presented a greater surface area to be cooled than any other component of the complete nozzle. Two outer-shell configurations were used. One outer shell was cooled by forced convection. The other was cooled with a corrugated louvered liner.

Plug requirements. - A typical variation of average plug surface temperature with plug cooling airflow for an exhaust-gas total temperature of 2550° F is shown in figure 12. A plug cooling airflow equal to 0.98 percent of the afterburner gas flow produced an average plug surface temperature of 1650° F. An increase in plug cooling airflow from 0.98 to 1.3 percent lowered the average surface temperature from 1650° to 1440° F.

The plug surface temperatures shown in figure 12 are averages of all the individual measurements on the plug surface. Average plug surface temperature is the average surface-area-weighted temperature over the plug surface. A typical variation of temperature along the plug surface is shown in figure 13. In this figure the vertical broken lines denote slot exits. Individual symbols are shown for the surface temperature at each circumferential location, and circumferential averages are shown by solid symbols.

A reason for the scatter of up to about 800° F in the circumferential plug surface temperature measurements at any given longitudinal station is shown by the light and dark patterns on the plug surface in figure 14, where the plug nozzle is shown during a typical afterburning run. The exhaust-gas total temperature and average plug surface temperature were 2837° F and 1587° F, respectively. Peculiarities of the fuel injection and combustion processes created hot streaks in the combustion gases and, hence, on the plug surface. The scatter of plug surface temperature, shown in figure 13, is also due in part to inherent circumferential and radial nonuniformities in the plug cooling airflow at each slot.

A typical distribution of plug cooling airflow (also, that which produced the plug surface temperature distribution of fig. 13) is shown in figure 15. Both cumulative and individual plug slot airflows are shown against plug surface area. The cumulative distribution was essentially constant for all the cooling data presented in this report. The vertical broken lines denote slot exits. The stagnation portion of the plug (nose) required more cooling per unit surface area than the tailcone (tip). About 51 percent of the cooling air (shown by the cumulative curve) was used ahead of the plug major diameter.

The sixth slot provided a large share of the total cooling airflow for the particular data of figure 15. This was not a necessary condition to produce safe plug surface temperatures on that portion of the plug. It is felt that the hypothetical redistribution of plug cooling airflow, shown by the dashed curve in figure 15, would represent a more general plug cooling-air design requirement. The plug surface temperature distribution accompanying this hypothetical change would probably be essentially that shown in figure 13.

Total (plug, struts, and outer-shell) requirements. - A summary of the cooling-air requirements for the complete nozzle (as well as the plug

cooling-air requirements) is shown in figure 16 for a range of exhaust-gas total temperatures from 1990° to 2840° F. A total cooling airflow of 4.5 percent of the afterburner gas flow at an exhaust-gas total temperature of 2840° F resulted in an average plug surface temperature of 1620° F. Additional curves show the cooling-air requirements at average plug surface temperature levels of 1520° and 1420° F. At an exhaust-gas temperature of 2480° F, the liner-cooled outer-shell lip temperature reached a limiting safe level, about 1940° F. Therefore, this outer shell was used only at exhaust-gas temperatures of less than 2480° F. The forced-convection film-cooled outer shell was used over the complete range of exhaust-gas temperatures investigated. The discontinuities in the curves showing the total requirements arise because the convection-cooled outer shell required no cooling airflow at exhaust-gas total temperatures below about 2480° F. The cooling air discharged from the corrugated liner of the main combustion chamber was helpful in cooling this outer shell.

A complete breakdown of the total cooling-air requirements for average plug surface temperatures of 1620°, 1520°, and 1420° F is shown in figures 17(a), (b), and (c), respectively. The average strut leading-edge temperatures were 1910°, 1799°, and 1693° F, respectively. The average temperatures of the convection-cooled outer-shell lip were 1286°, 1262°, and 1209° F, respectively. In figure 17(a), the total nozzle cooling airflow of 4.5 percent of the afterburner gas flow at the exhaust gas total temperature of 2840° F comprised about 1.2 percent for plug cooling, 2.6 percent for plug-support strut cooling, and 0.7 percent for outer-shell cooling. From figure 17 it is apparent that the struts required about twice as much cooling air as the plug. Calculations show that the strut cooling-air requirements could be reduced by redesign of the strut cooling passages to improve their forced-convection cooling characteristics. The strut cooling-air requirements could be reduced by at least 50 percent. For example, at an exhaust-gas total temperature of 2840° F, the total cooling-air requirements would be reduced to about 3.2 percent of the afterburner gas flow if the average plug surface temperature were maintained at 1620° F.

Internal Thrust

Investigation of the internal-thrust performance of the plug nozzle included the effects of exhaust-nozzle pressure ratio, plug tailcone roughness, and cooling airflow on jet-thrust coefficient.

Effect of exhaust-nozzle pressure ratio. - The value of jet-thrust coefficient was constant at about 0.97 for the full-scale plug nozzle (with smooth tailcone) over a range of exhaust-nozzle pressure ratios from about 1.5 to 10.8 and for area ratios of 1.50 and 1.85, as shown in figure 18. The data for a similar model plug nozzle (ref. 1) is shown as a shaded band and agrees well with the full-scale data. Any evidence that

the full-scale jet-thrust coefficient reached a maximum value at its design pressure ratio was masked by the scatter of the data and by the small number of data points available. The internal, off-design, thrust performance of the nozzle would be compromised by jet interaction with an external stream as shown in reference 7. However, the plug nozzle still appears attractive for applications requiring good thrust over a broad range of pressure ratios.

Effect of plug tailcone roughness. - Figure 19 shows the adverse effect of plug surface roughness on jet-thrust coefficient for area ratios of 1.50 and 1.85. The loss in jet-thrust coefficient amounted to about 2 percent at an area ratio of 1.85. Where less of the tailcone surface area was exposed to supersonic flow (i.e., area ratio of 1.50), the loss was only about 1 percent. An illustration of the plug surface roughness is shown in figure 20. The dashed lines indicate the original profile of the plug surface in several circumferential locations. The solid lines, obtained from clay impressions, show the rough (buckled) surface condition. The buckles resulted from relief of thermal stresses in the plug skin.

Effect of cooling airflow. - There were no significant favorable or adverse effects of cooling airflow (either from the plug slots or the struts) on jet-thrust coefficient. The effect of plug cooling airflow is shown in figure 21, where the jet-thrust coefficient was constant for ratios of plug cooling airflow to afterburner gas flow up to about 0.028. Figure 22 shows the effect of strut cooling airflow. The jet-thrust coefficient was again constant for ratios of strut cooling airflow to afterburner gas-flow up to about 0.016. In addition, figure 22 demonstrates the adverse effect of plug surface roughness.

SUMMARY OF RESULTS

The cooling requirements and internal thrust performance of an air-cooled, plug-type, variable-area exhaust nozzle were experimentally investigated in a turbojet-engine afterburner over a range of exhaust-gas total temperatures from 1990° to 2840° F and a range of exhaust-nozzle pressure ratios from 1.5 to 10.8.

At a typical exhaust-gas total temperature of 2550° F and a cooling-air temperature of 78° F, a plug cooling airflow of 0.98 percent of the afterburner gas flow produced an average plug surface temperature of about 1650° F. Increasing the plug cooling airflow to 1.3 percent of the afterburner gas flow reduced the average plug surface temperature to 1440° F. At the highest exhaust-gas total temperature investigated (2840° F), a total-nozzle cooling airflow of 4.5 percent of the afterburner gas flow produced an average plug surface temperature of 1620° F. The value of 4.5 percent comprised about 1.2 percent for plug cooling, 2.6 percent for plug support-strut cooling, and 0.7 percent for outer-shell cooling.

[redacted]

The value of jet-thrust coefficient was constant at about 0.97 over a range of exhaust-nozzle pressure ratios from 1.5 to 10.8 for the full-scale plug nozzle with a smooth fairing on the tailcone. This level of internal-thrust performance agreed well with prior NACA model-plug-nozzle data. A loss in jet-thrust coefficient of up to 2 percent was caused by roughness (discontinuities and buckles) on the plug tailcone surface.

Lewis Flight Propulsion Laboratory
National Advisory Committee for Aeronautics
Cleveland, Ohio, January 8, 1957

APPENDIX A

SYMBOLS

A	cross-sectional area, sq ft
C	coefficient
F	thrust, lb
g	acceleration due to gravity, ft/sec^2
h	heat-transfer coefficient evaluated at film temperature, $Btu/(hr)(sq\ ft)(^oF)$
$K_0(\ ), K_1(\ )$	modified Bessel functions of second kind of order n
k	thermal conductivity, $Btu/(hr)(sq\ ft)(^oF/ft)$
L	length of swaged thermocouple exposed to cooling airflow, ft
l	perimeter, ft
P	total pressure, lb/sq ft abs
p	static pressure, lb/sq ft abs
R	gas constant, $ft\text{-}lb/(lb)(^oR)$
r	radius, ft
T	total temperature, ^oF
t	thickness, ft
w	weight-flow rate, lb/sec
γ	ratio of specific heats

Subscripts:

AB	afterburner
a	air or air side
an	annulus in plane of outer-shell lip
b	compressor overboard bleed
e	engine
ex	exhaust
F	jet thrust
f	fuel
g	gas or gas side
i	indicated thermocouple junction
j	jet
l	thermocouple lead
p	plug, upstream of plane of outer-shell lip
sk	skin
st	strut
1	engine inlet
2	turbine discharge
3	afterburner, exhaust-nozzle inlet
4	plane of outer-shell lip
∞	infinitely removed from heat sink (thermocouple lead)

Superscript:

'	ideal

[redacted]

APPENDIX B

CALCULATIONS

Cooling airflow. - Cooling airflows to each of the plug slots, the struts, and the convection-cooled outer shell were measured individually by passing each flow through a separate calibrated pipe.

Exhaust-nozzle gas flow. - Gas flow through the exhaust nozzle was defined as the mass flow passing through the nozzle throat (arbitrarily assumed as the annular flow passage coplanar with the lip of the outer shell). That is,

$$w_{g,4} = w_{a,l} - w_{a,b} + w_{f,e} + w_{f,AB} + w_{a,st} + w_{a,p}$$

where

$w_{a,st}$ strut cooling airflow (discharged directly into afterburner at outer ends of struts)

$w_{a,p}$ plug-slot cooling airflow for slots discharging into exhaust gas upstream of throat

Jet-thrust coefficient. - The jet-thrust coefficient was defined as the ratio of actual jet thrust to ideal jet thrust, or

$$C_F = \frac{F_j}{F'_j} = \frac{F_j}{w_{g,4}\sqrt{\frac{2R_4(T_4 + 460)}{g}\frac{\gamma_4}{(\gamma_4 - 1)}\left[1 - \left(\frac{p_{ex}}{P_3}\right)^{\frac{\gamma_4 - 1}{\gamma_4}}\right]}}$$

Exhaust-gas total temperature. - For nonafterburning conditions it was assumed (and experimentally verified) that the average total temperature at station 3 was nearly equal to the average turbine-discharge total temperature. Thus, the ideal jet thrust and jet-thrust coefficient could be computed for nonafterburning conditions. For afterburning calculations, the jet-thrust coefficient was assumed equal to the value from the nonafterburning calibration at the same operating pressure ratio and area ratio. Then T_4 was computed using the following definition of jet-thrust coefficient:

$$T_4 = \left[\frac{F_j}{C_F w_{g,4}}\right]^2 \frac{g}{2R_4\left(\frac{\gamma_4}{\gamma_4 - 1}\right)\left[1 - \left(\frac{p_{ex}}{P_3}\right)^{\frac{\gamma_4 - 1}{\gamma_4}}\right]} - 460^\circ$$

Swaged-thermocouple corrections. - For ease of fabrication, the swaged-type thermocouples were welded normal to a surface. Cooling air then flowed over the swaged tubing. This type of installation resulted in the local depression of thermocouple-junction temperatures of up to several hundred degrees, inasmuch as the thermocouple junction was in the center of the surface area being cooled by the lead. A theoretical analysis of this pin-fin-type cooling has been made in reference 7, where it is shown that the temperature depression due to the presence of the cooled thermocouple lead may be expressed as

$$T_\infty - T_i = \left[\frac{\lambda(T_i - T_a)\tanh mL - (T_4 - T_i)}{2\pi r_l t_{sk} k_{sk} \sqrt{\beta}}\right] \frac{K_0(\sqrt{\beta}\, r_L)}{K_1(\sqrt{\beta}\, r_L)}$$

where

T_∞ true skin temperature in absence of cooling effect of thermocouple lead, °F

T_i indicated skin temperature at thermocouple junction, °F

T_a total temperature of air cooling thermocouple lead, °F

T_4 exhaust-gas total temperature near thermocouple junction, °F

λ $\sqrt{h_L l_L k_L A_L} = \pi r_L \sqrt{2 r_L h_L k_L}$

m $\sqrt{\frac{h_L l_L}{k_L A_L}} = \sqrt{\frac{2h_L}{k_L r_L}}$

α $h_g A_L = h_g \pi r_L^2$

β $\frac{h_a + h_g}{t_{sk} k_{sk}}$

[redacted]

These equations were used to correct all the swaged-thermocouple readings subject to the pin-fin-type cooling in this report.

An alternate method of installing the thermocouples to avoid this local temperature depression of the junction would have been to imbed the lead in the wall with the thermocouple junction far enough removed radially (about 0.5 in. in this case) to be out of the area of influence of the pin fin (i.e., essentially at T_∞). However, the installation of imbedded thermocouples in the plug surface would have been prohibitively tedious because of the limited working volume and the inaccessibility of the plug interior.

REFERENCES

1. Krull, H. George, Beale, William T., and Schmiedlin, Ralph F.: Effect of Several Design Variables on Internal Performance of Convergent-Plug Exhaust Nozzles. NACA RM E56G20, 1956.

2. Krull, H. George, and Beale, William T.: Effect of Outer-Shell Design on Performance Characteristics of Convergent-Plug Exhaust Nozzles. NACA RM E54K22, 1955.

3. Krull, H. George, and Beale, William T.: Comparison of Two Methods of Modulating the Throat Area of Convergent Plug Nozzles. NACA RM E54L08, 1955.

4. Steffen, Fred W., Krull, H. George, and Schmiedlin, Ralph F.: Effect of Divergence Angle on the Internal Performance Characteristics of Several Conical Convergent-Divergent Nozzles. NACA RM E54H25, 1954.

5. Ciepluch, Carl C., Krull, H. George, and Steffen, Fred W.: Preliminary Investigation of Performance of Variable-Throat Extended-Plug-Type Exhaust Nozzles over Wide Range of Pressure Ratios. NACA RM E53J28, 1954.

6. Salmi, R. J., and Cortright, E. M., Jr.: Effects of External Stream Flow and Afterbody Variations on the Performance of a Plug Nozzle at High Subsonic Speeds. NACA RM E56F11a, 1956.

7. Boelter, L. M. K., Cherry, V. H., Johnson, H. A., and Martinelli, R. C.: Heat Transfer Notes. Ch. IIb-18, Univ. Calif. Press (Berkeley and Los Angeles), 1948.

[redacted]

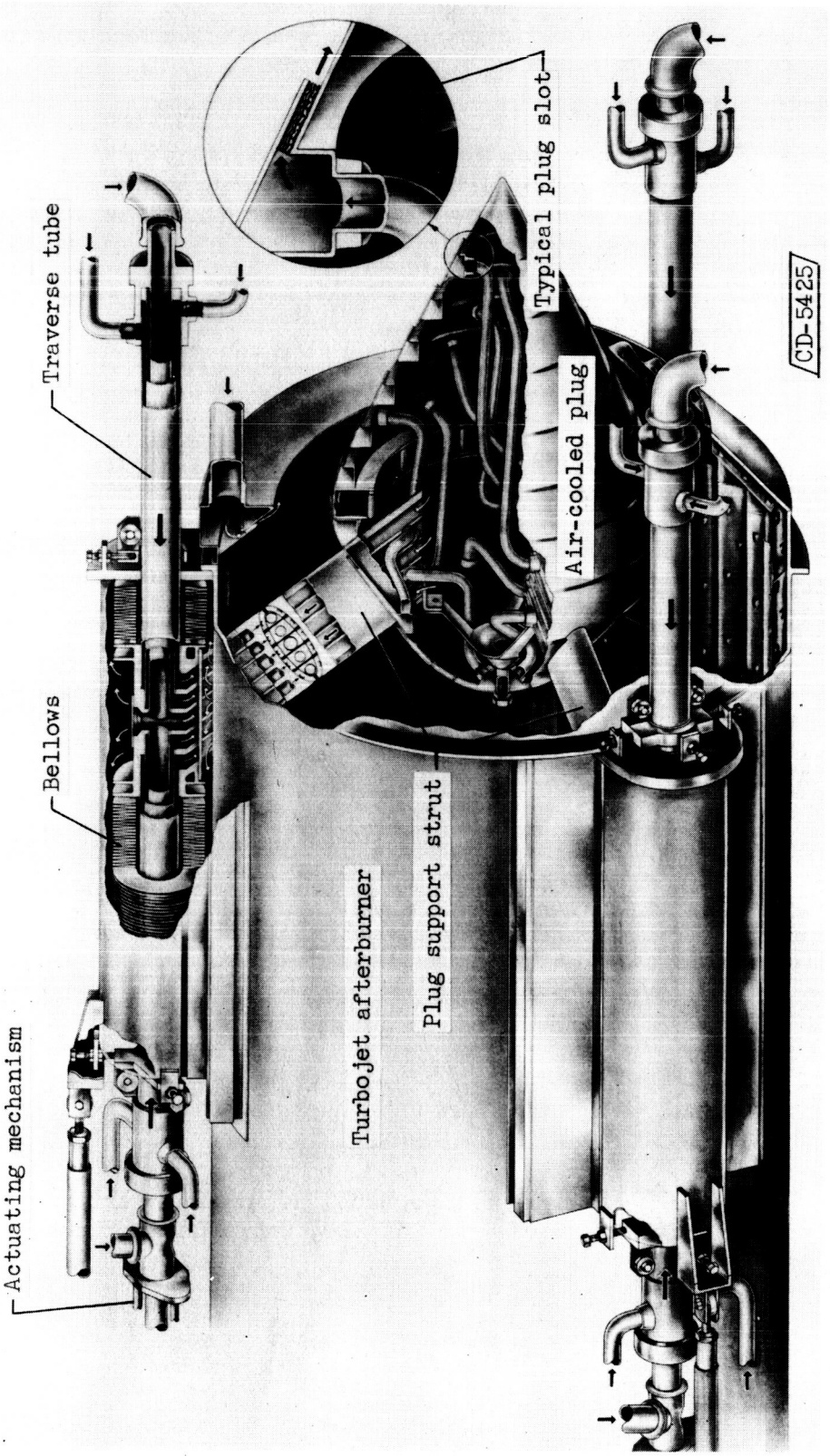

(a) Exhaust nozzle installed in afterburner.

Figure 1. - Air-cooled, plug-type, variable-area, exhaust nozzle.

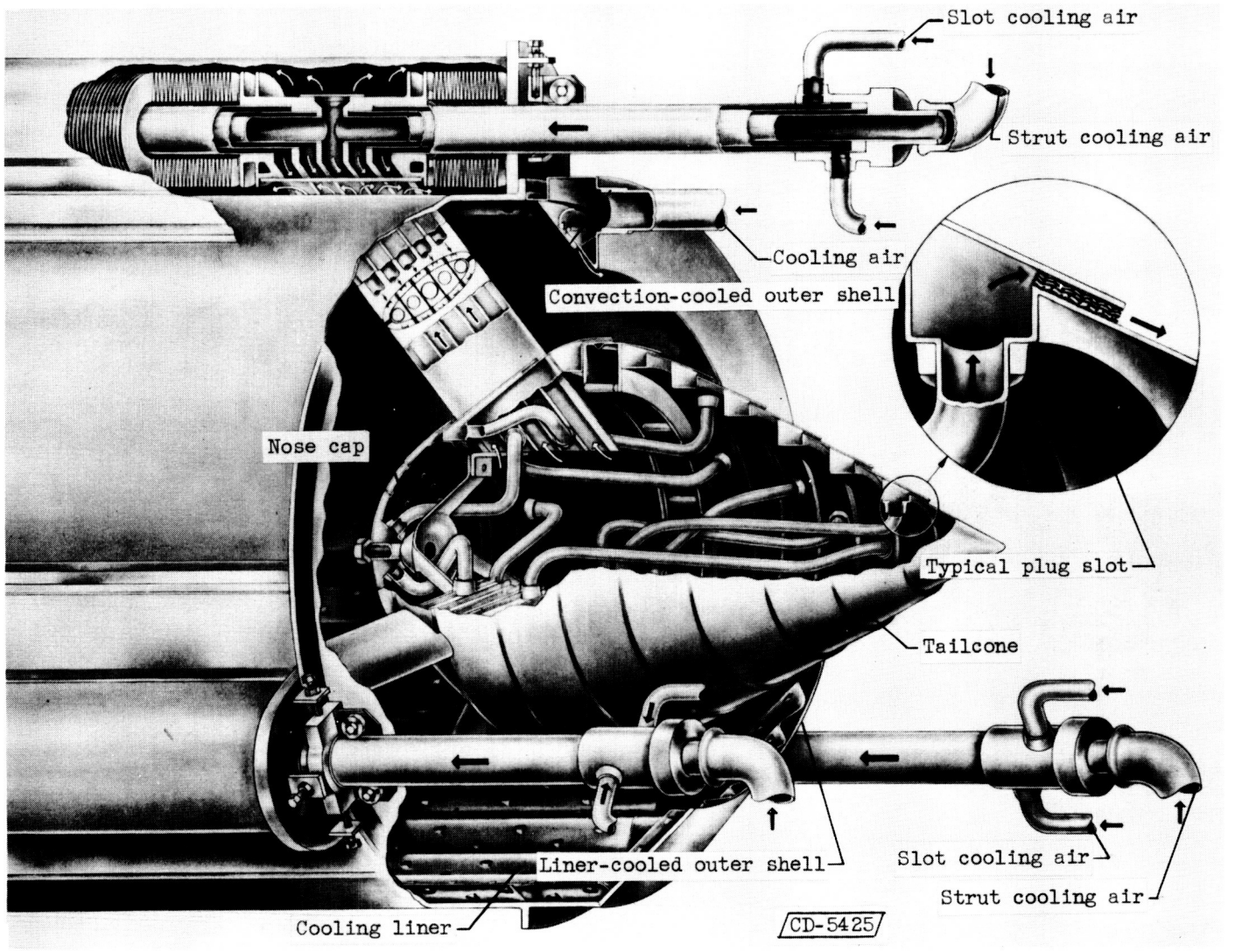

(b) Plug-nozzle cooling systems.

Figure 1. - Concluded. Air-cooled, plug-type, variable-area, exhaust nozzle.

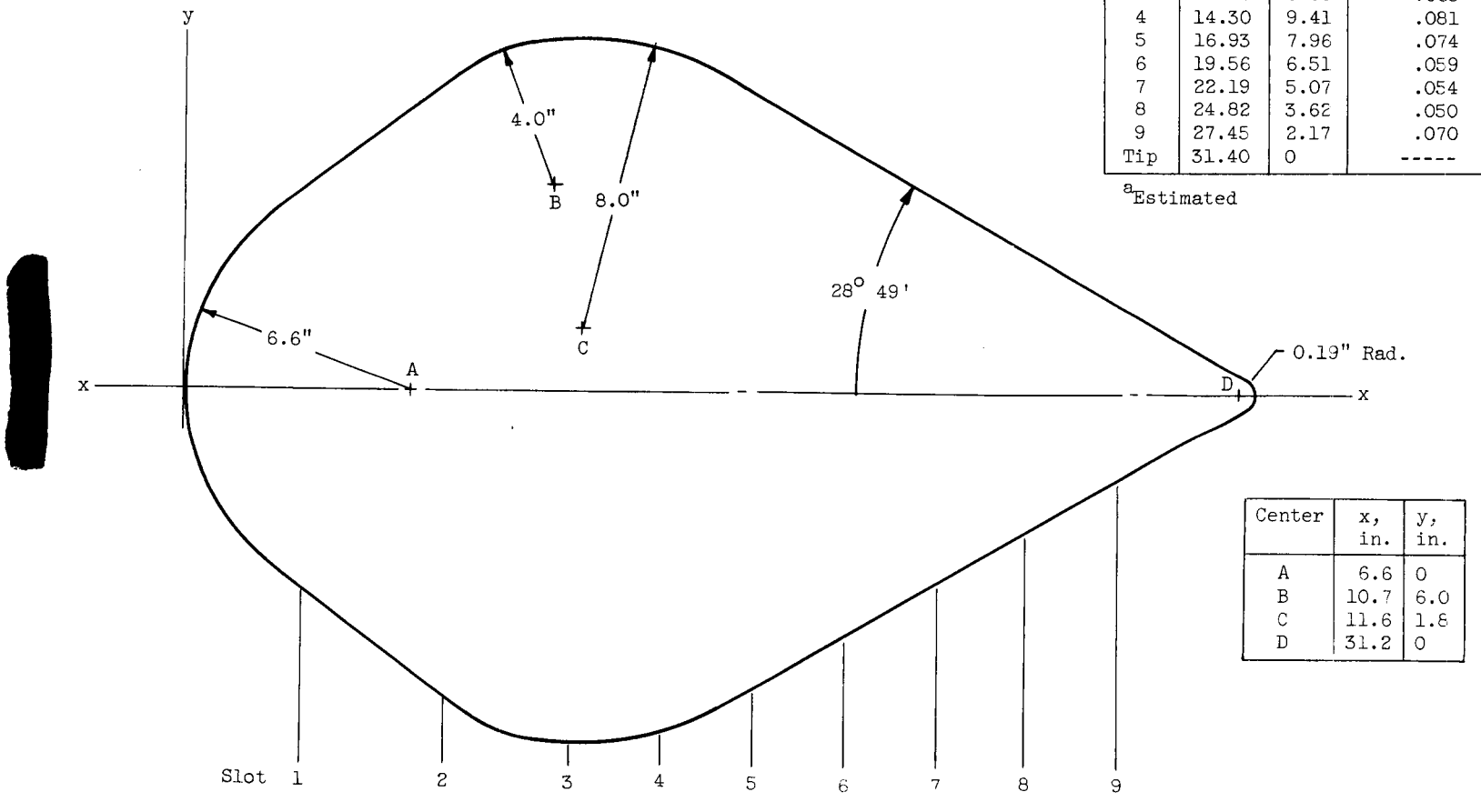

Slot	x, in.	y, in.	Net initial slot height, in.
1	3.90	6.10	[a]0.065
2	8.10	9.30	[a].065
3	11.70	10.00	[a].065
4	14.30	9.41	.081
5	16.93	7.96	.074
6	19.56	6.51	.059
7	22.19	5.07	.054
8	24.82	3.62	.050
9	27.45	2.17	.070
Tip	31.40	0	-----

[a]Estimated

Center	x, in.	y, in.
A	6.6	0
B	10.7	6.0
C	11.6	1.8
D	31.2	0

Figure 2. - Plug profile envelope dimensions.

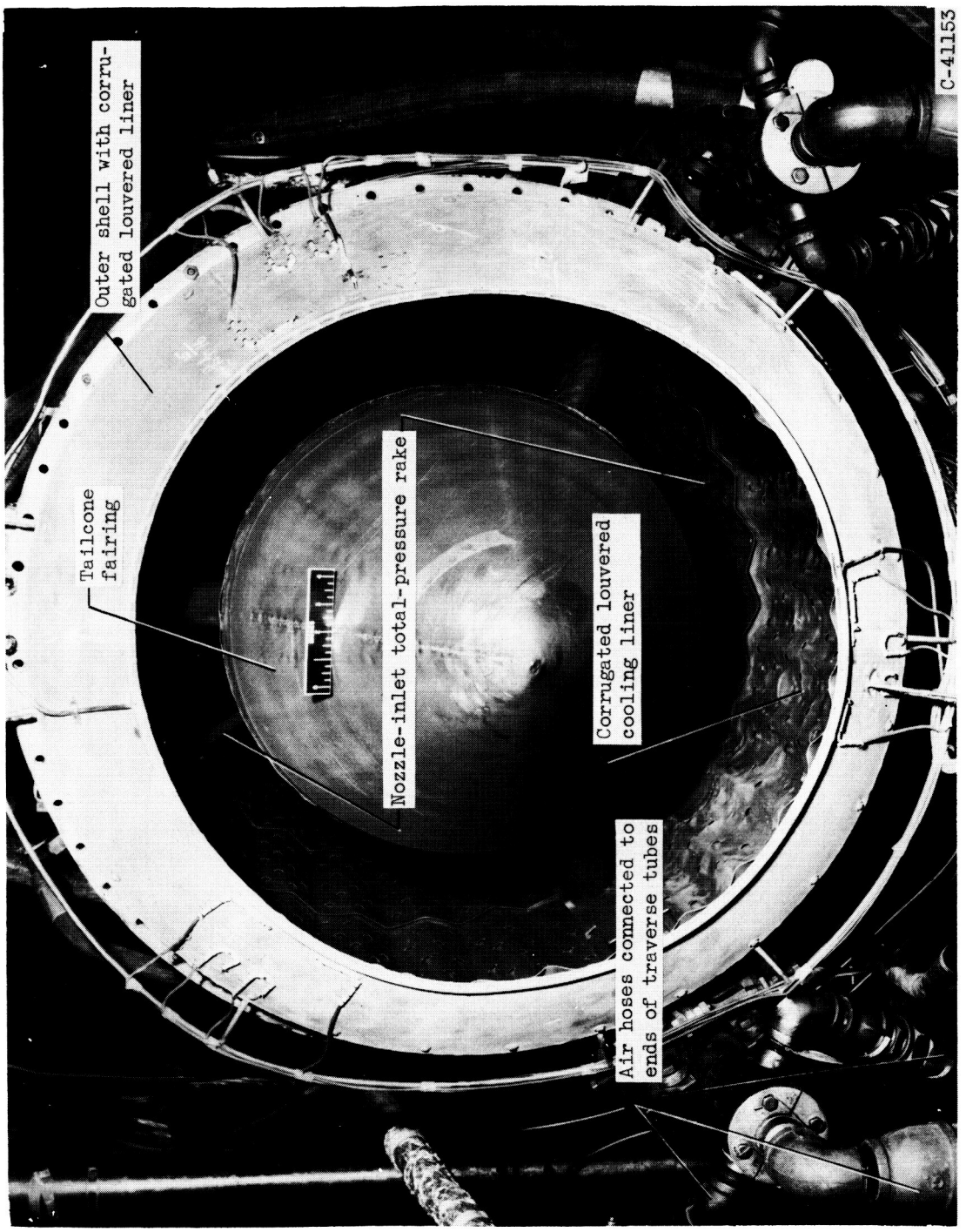

Figure 3. - Plug nozzle with smooth fairing covering tailcone.

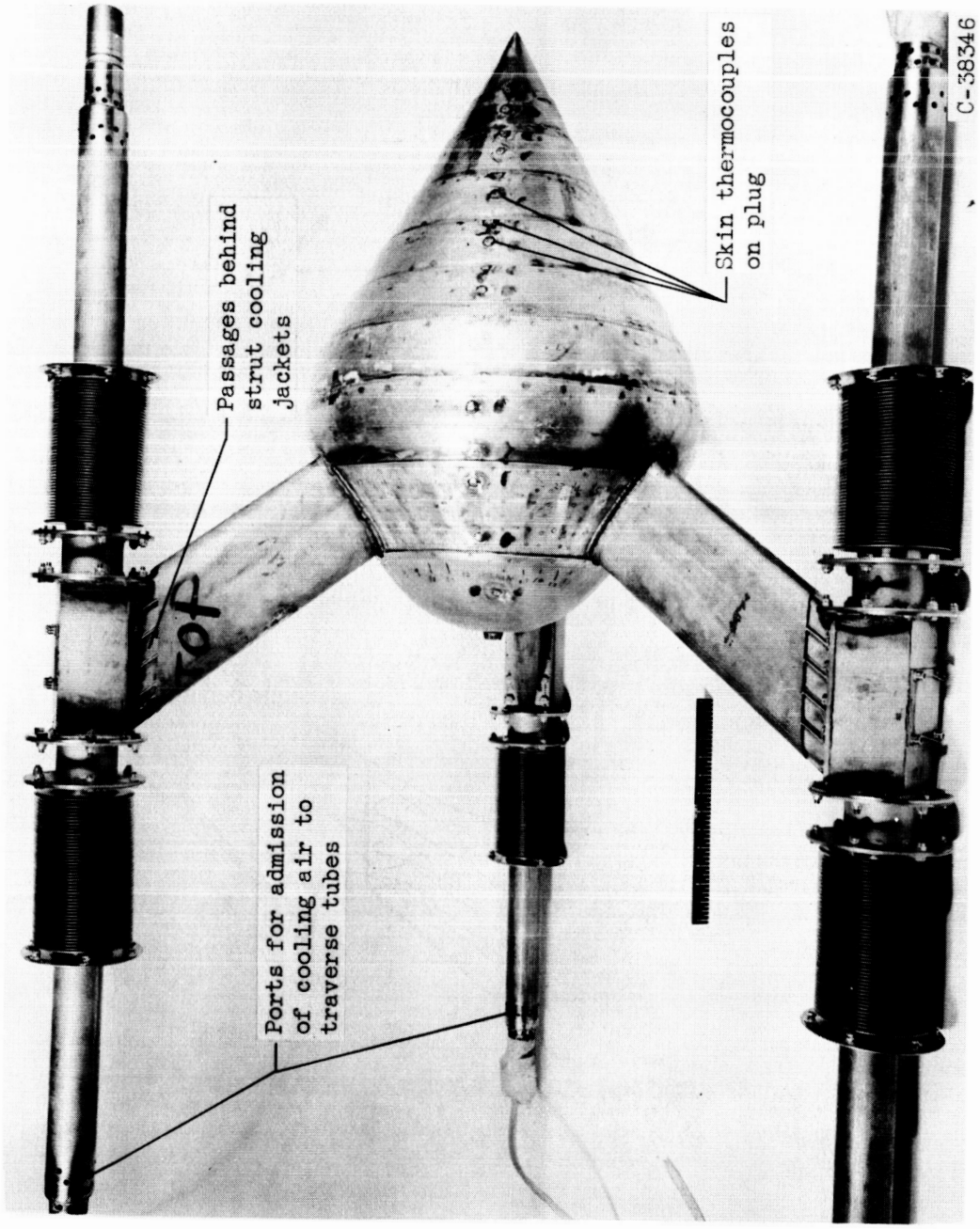

Figure 4. - Plug and traverse tube assembly.

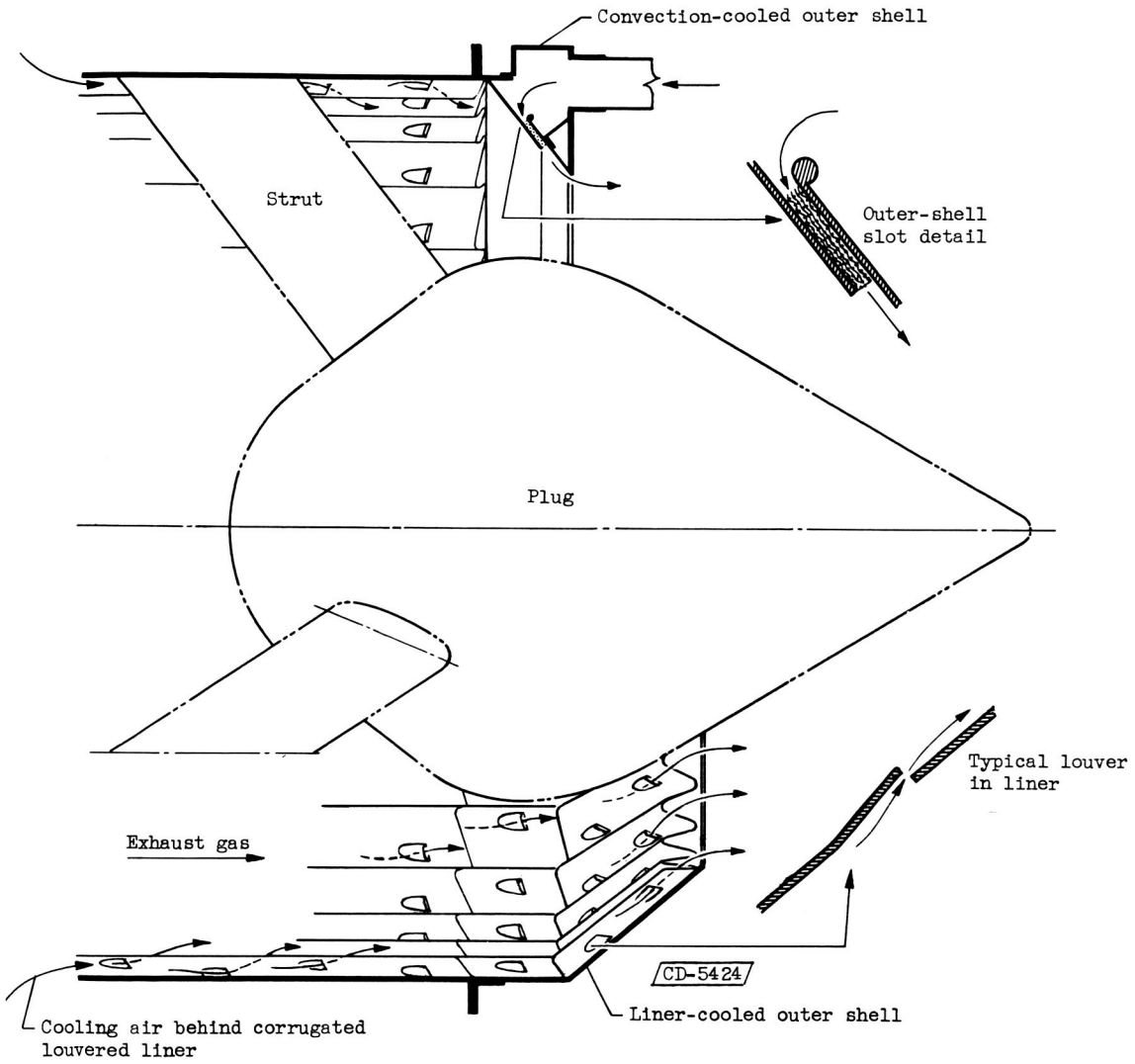

Figure 5. - Plug nozzle showing outer-shell cooling methods.

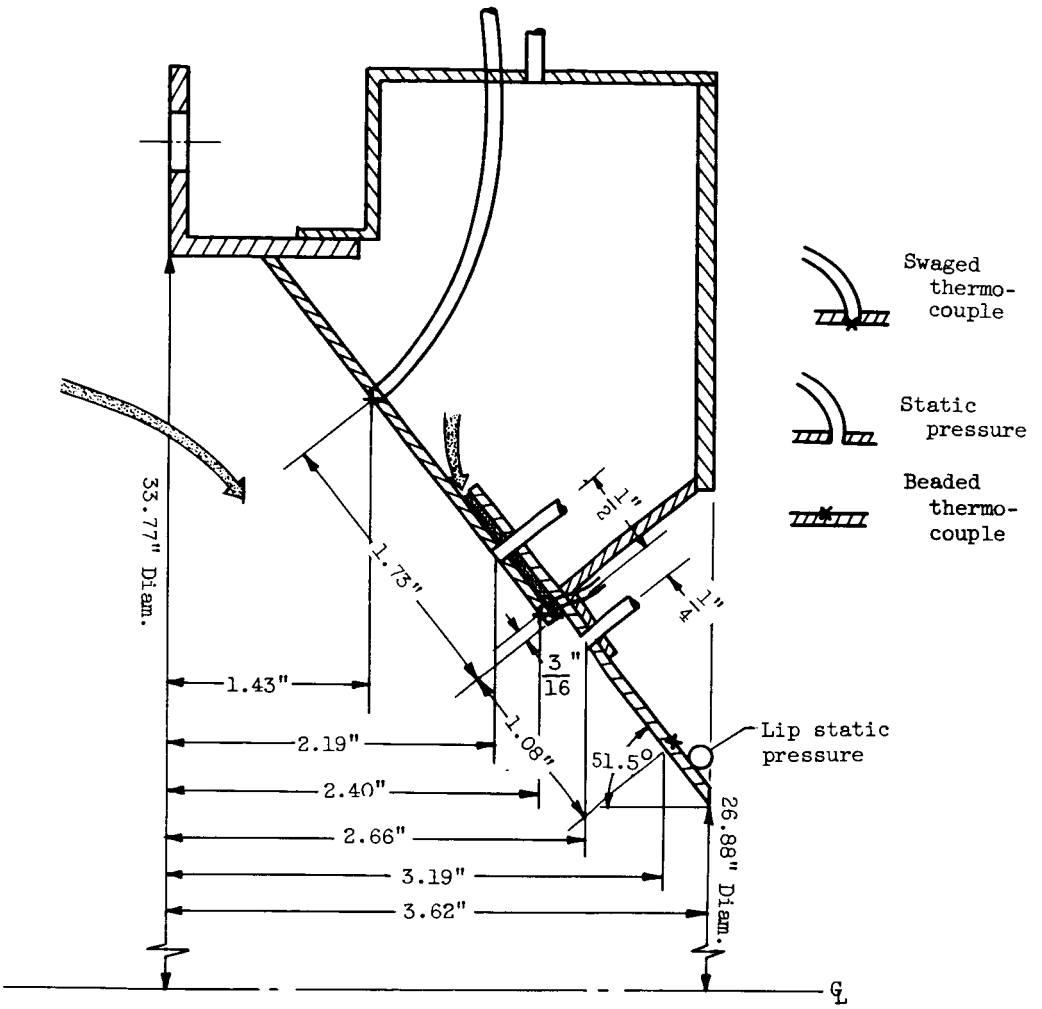

Instrumentation Details

Longitudinal location, in.	Circumferential location, deg[a]	Type
1.43	60,180,300	Skin thermocouple
2.19	300	Wall static pressure
2.40	60,180,300	Skin thermocouple
2.40	90	Wall static pressure
2.66	300	Wall static pressure
3.19	60,180,300	Skin thermocouple
3.62	120,300	Lip static pressure

[a]Clockwise from top looking downstream

(a) Forced-convection film-cooled outer shell.

Figure 6. - Plug-nozzle outer shells.

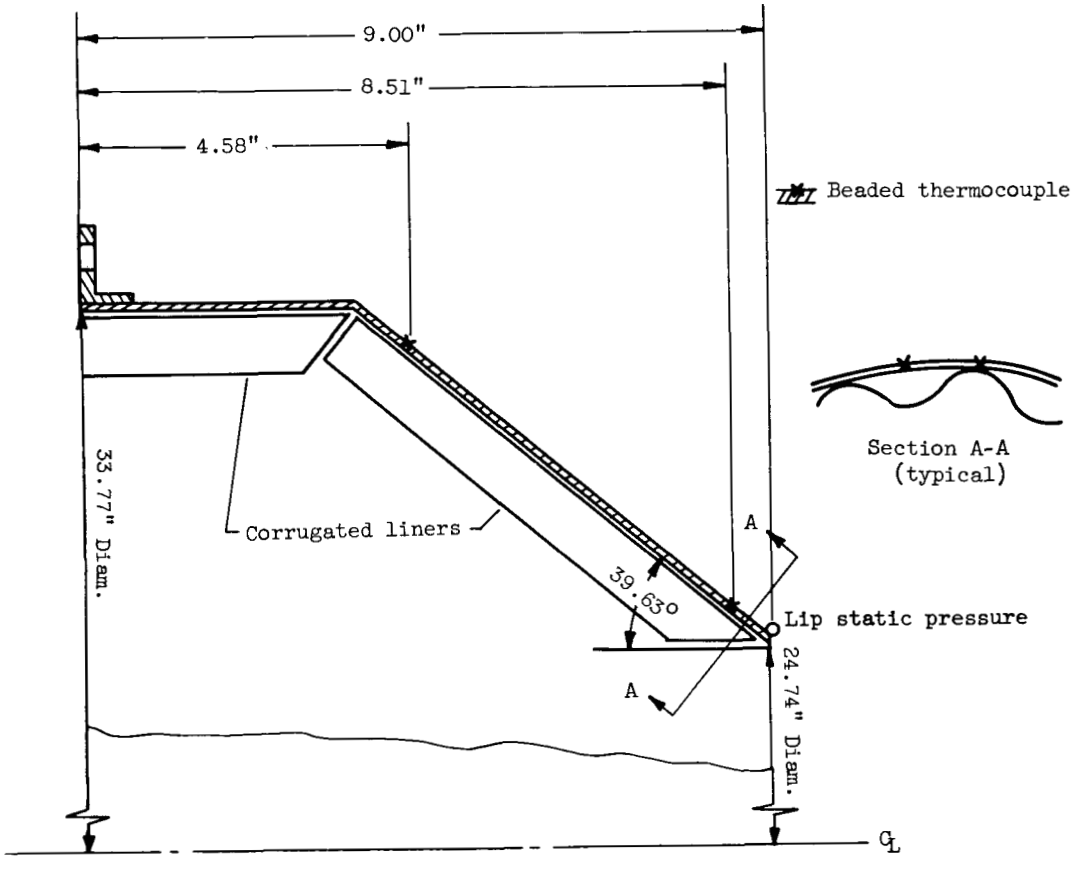

Instrumentation Details

Longitudinal location, in.	Circumferential location, deg[a]	Type
4.58	54,174,294 60,180,300	Skin thermocouple
9.00	120,300	Lip static pressure

[a]Clockwise from top looking downstream

(b) Outer shell cooled with corrugated louvered liner.

Figure 6. - Concluded. Plug-nozzle outer shells.

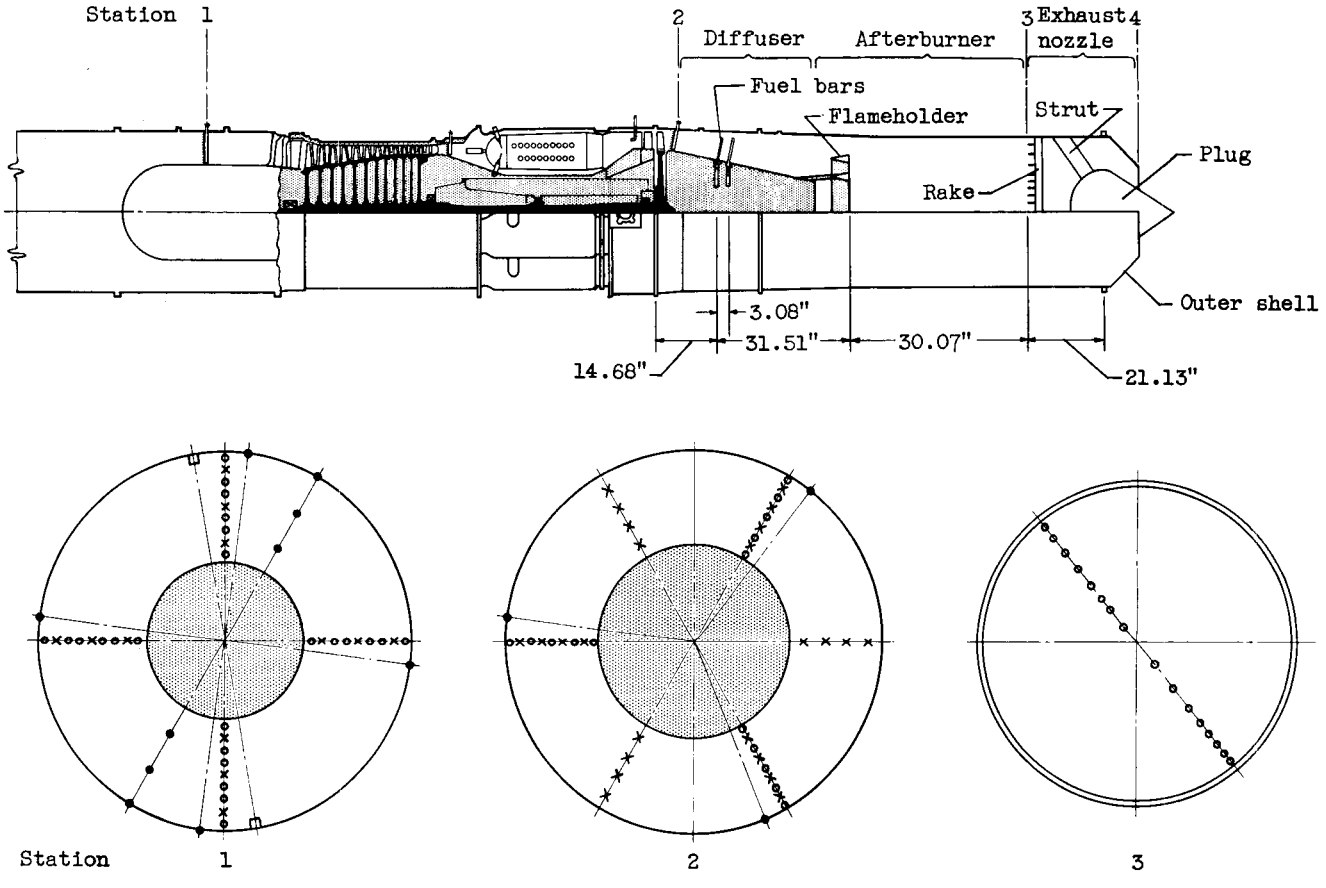

Figure 7. - Schematic diagram of turbojet-afterburner combination equipped with air-cooled, plug-type, variable-area exhaust nozzle.

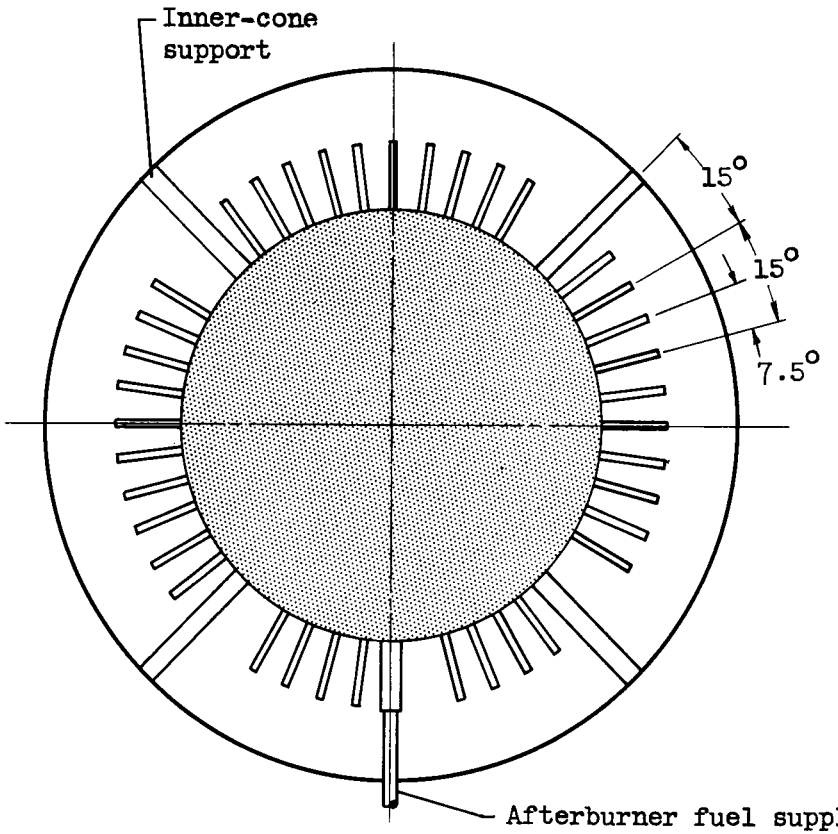

(a) Circumferential location of spray bars.

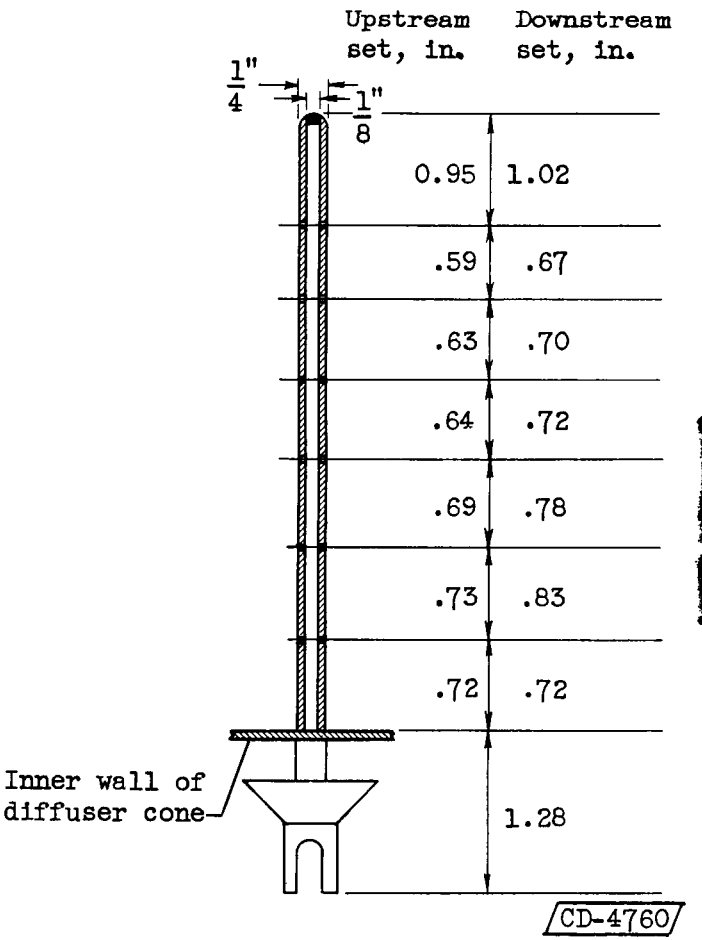

(b) Hole spacing of fuel spray bars.

Figure 8. - Fuel-system details.

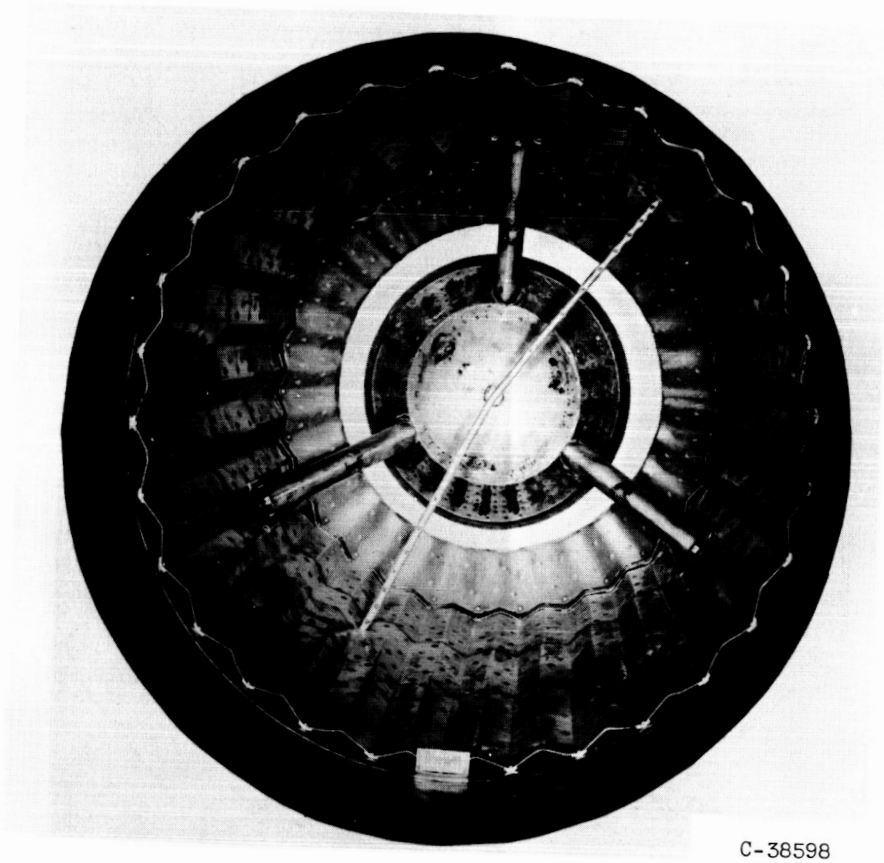

C-38598

Figure 9. - Interior view of plug-nozzle afterburner showing antiscreech cooling liner.

Location	Circumferential location, deg.		
	60	180	300
	Instrumentation[a]		
0a			TP
0b	T	T	TP
1a	T		TP
1b	T		T
1c			P
2a	T		TP
2b	T	T	TP
3a			TP
3b	T	T	T
3c	T		TP
4a			TP
4b	T	T	T
4c	T		TP
5a			TP
5b	T	T	T
5c	T		TP
6a			TP
6b	T		T
6c	T		TP
7a			TP
7b	T		T
7c	T		TP
8a			TP
8b	T		T
8c	T		TP
9a			TP
9b			T
9c			TP

[a]T, Swaged thermocouple;
P, static-pressure tap.

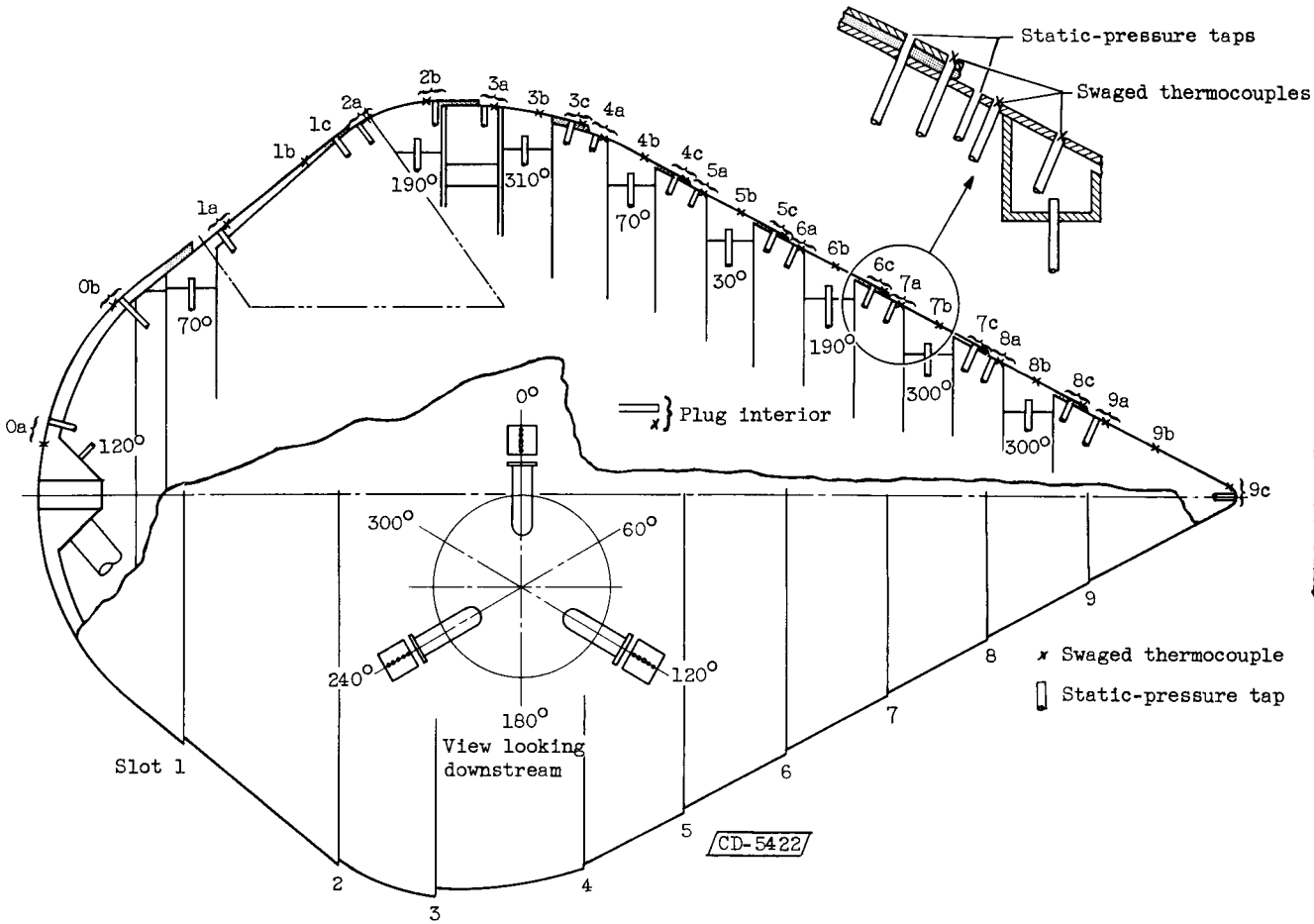

Figure 10. - Plug instrumentation and internal construction.

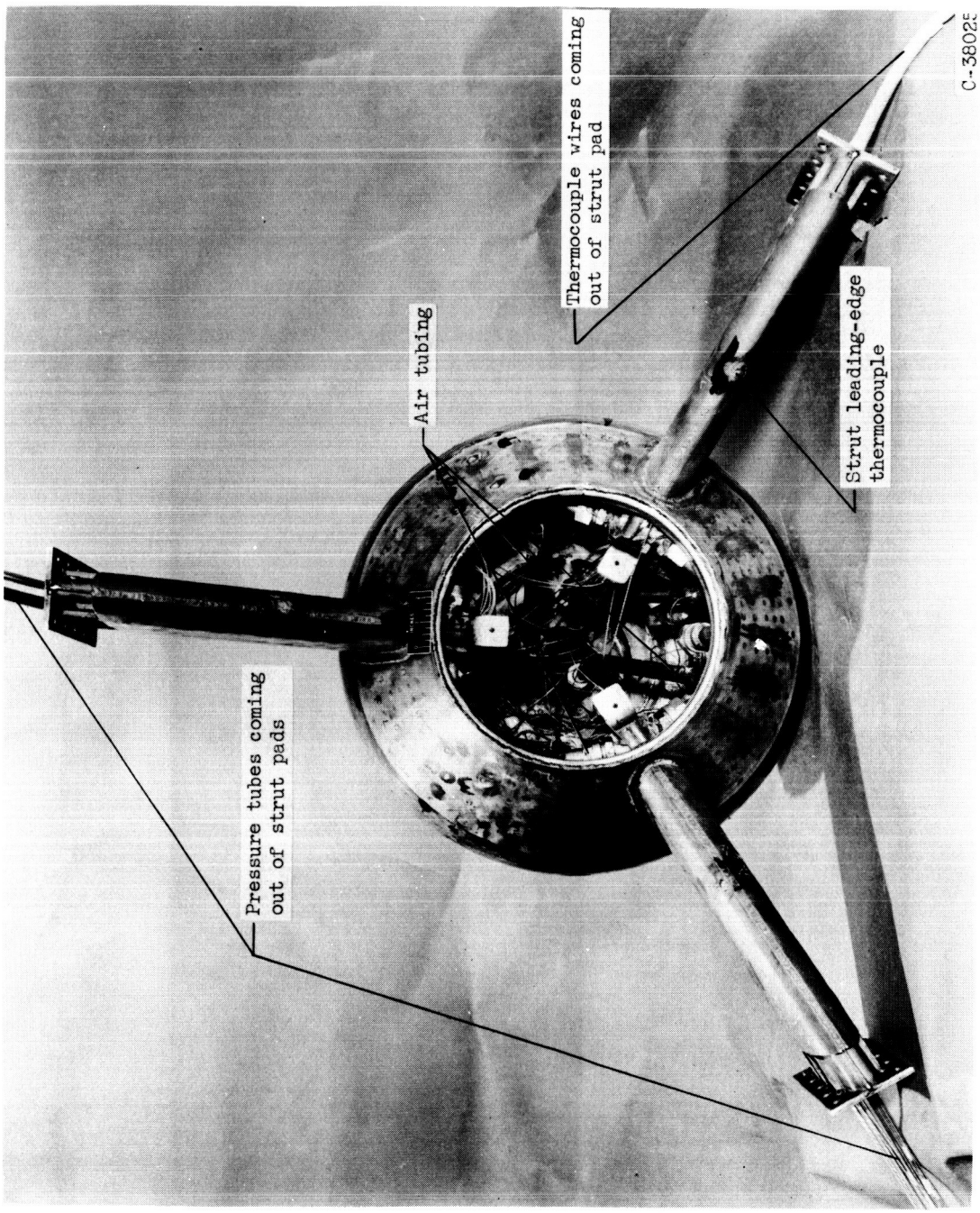

Figure 11. - Tail plug with nose cap removed to show instrumentation and cooling-air tubing.

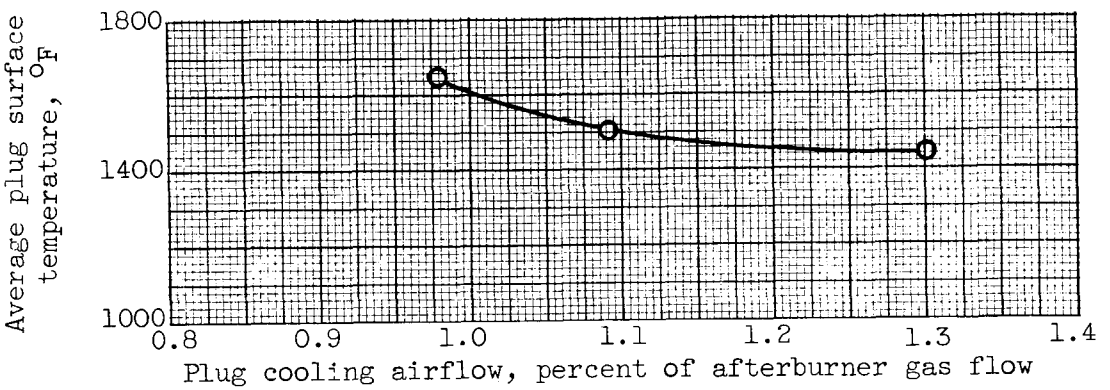

Figure 12 - Typical variation of average plug surface temperature with plug cooling airflow. Average exhaust gas total temperature, 2550° F, average cooling air temperature, 78° F.

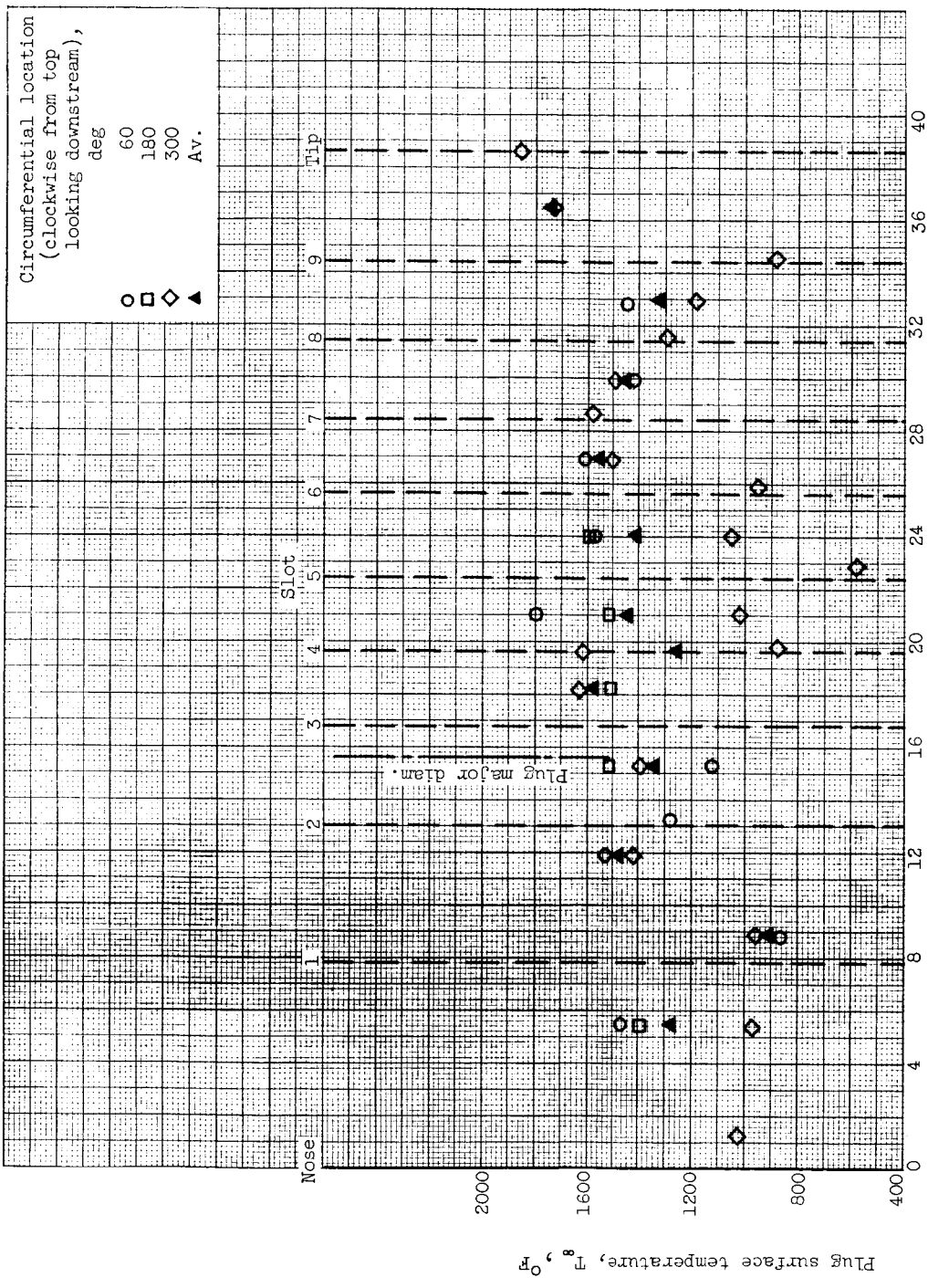

Figure 13. - Typical plug surface temperature distribution. Exhaust-gas temperature, 2585° F; weighted average plug surface temperature, 1437° F; cooling-air temperature, 86° F; total nozzle cooling airflow, 3.97 percent of afterburner gas flow; afterburner total pressure, 3644 pounds per square foot absolute; pressure ratio, 1.76; afterburner gas flow, 83.19 pounds per second.

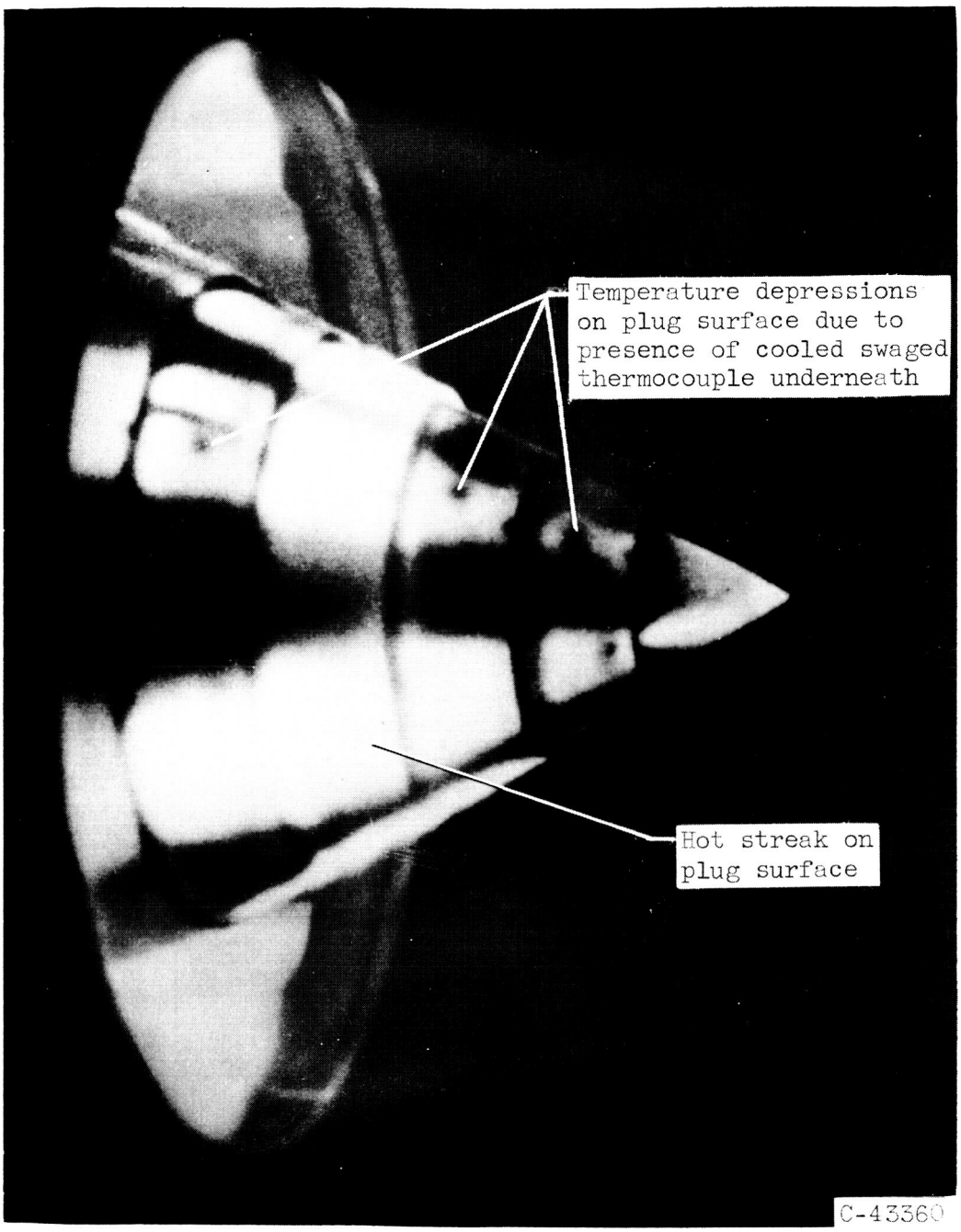

Figure 14. - Plug nozzle during afterburning operation. Exhaust-gas temperature, 2837°F.

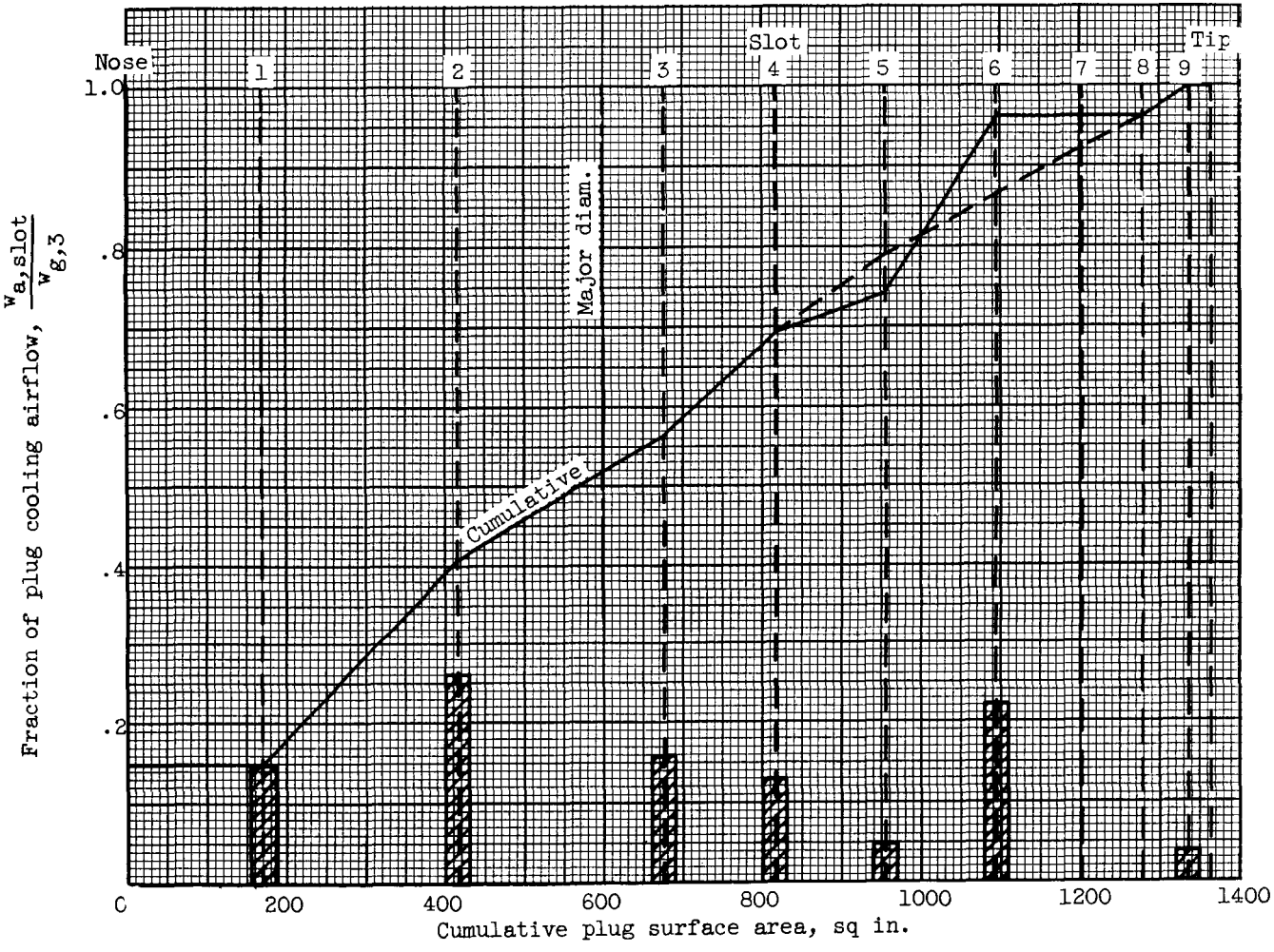

Figure 15. - Typical plug airflow distribution. Average plug surface temperature, 1437° F; exhaust-gas temperature, 2585° F; cooling-air temperature, 86° F; afterburner total pressure, 3644 pounds per square foot absolute; afterburner total-pressure ratio, 1.761; afterburner gas flow, 83.19 pounds per second; total nozzle cooling airflow, 3.87 percent of afterburner gas flow.

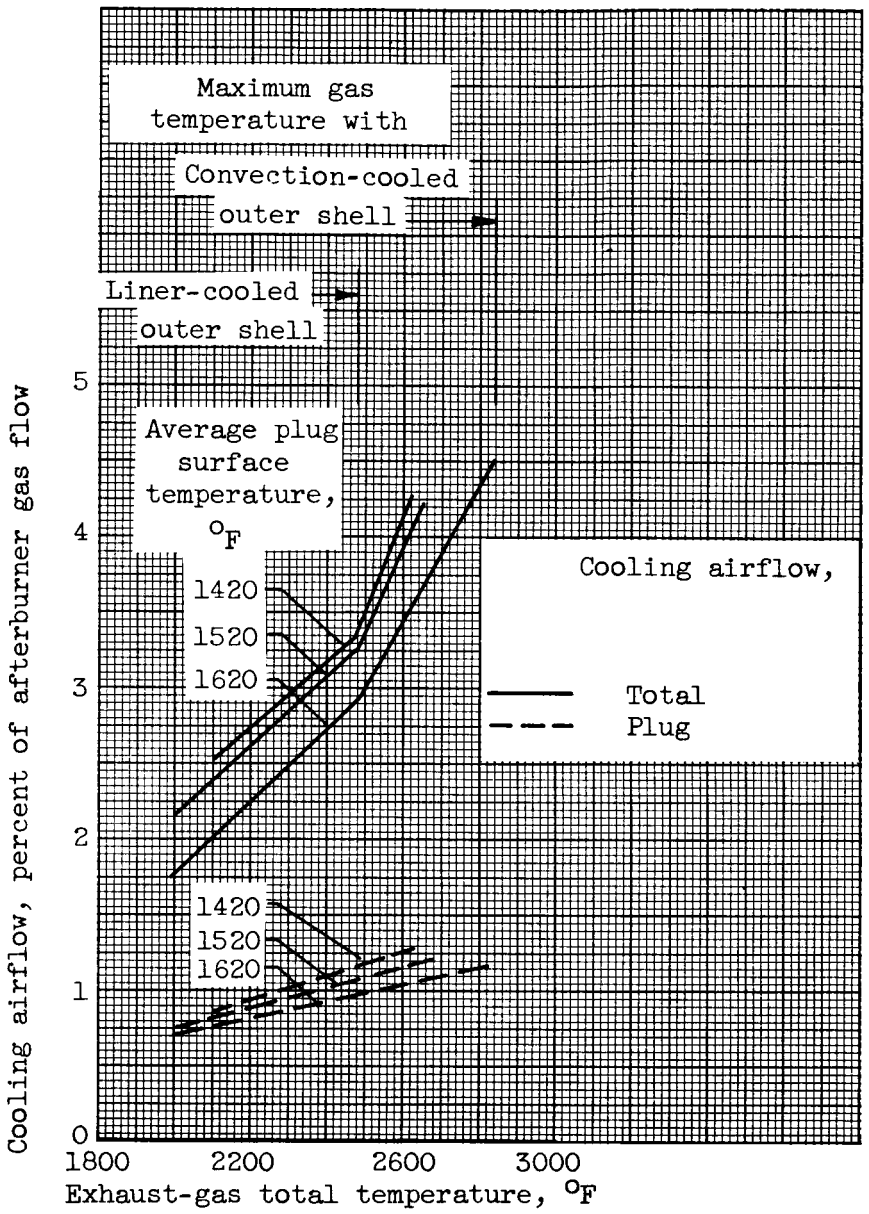

Figure 16. - Complete nozzle cooling-air requirements. Average afterburner total pressure, 4005 pounds per square foot absolute; average exhaust gas flow, 101.56 pounds per second; average cooling-air temperature, 78° F.

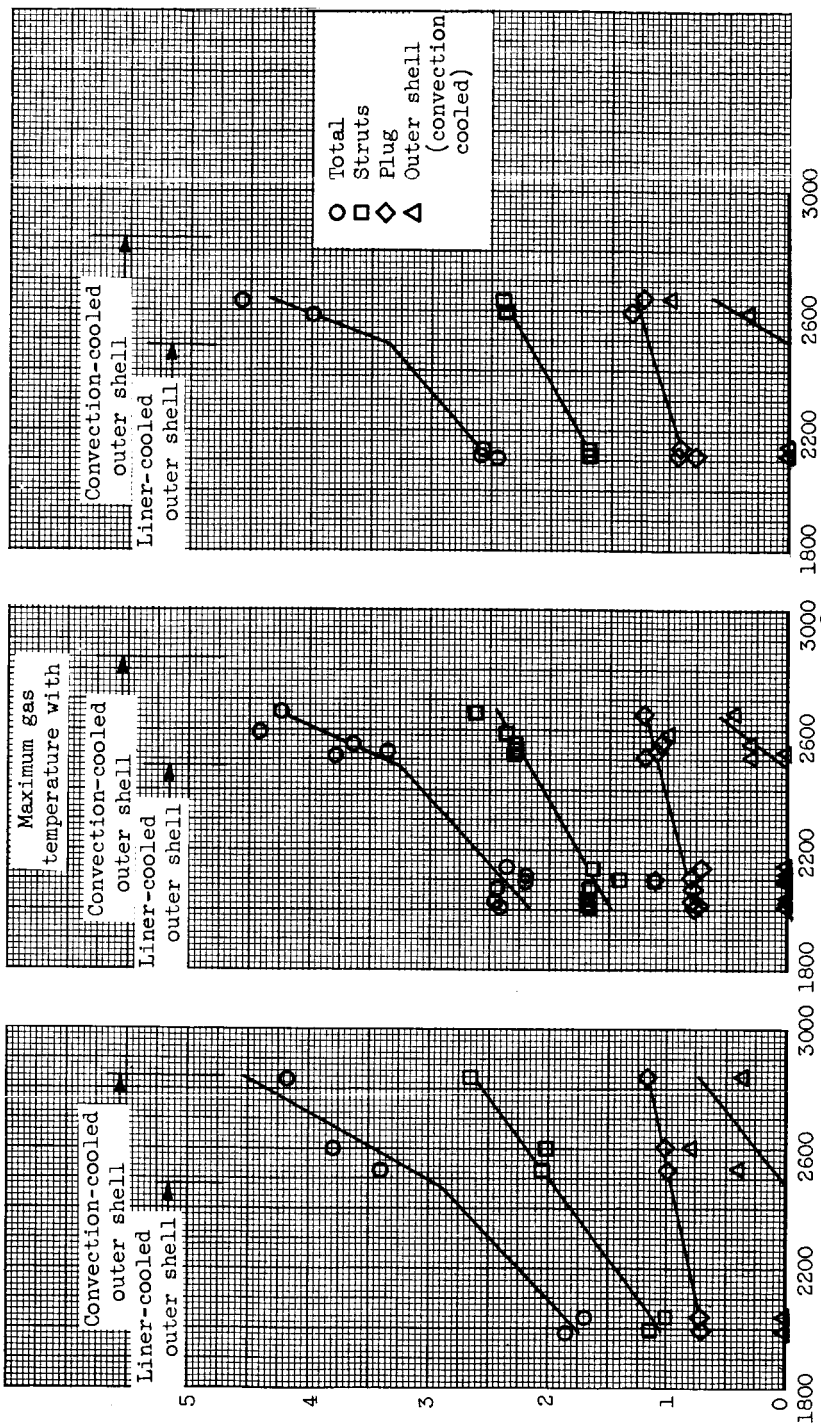

(a) Average plug surface temperature, 1620° F; average strut leading-edge temperature, 1910° F; average outer-shell lip temperature, 1286° F.

(b) Average plug surface temperature, 1520° F; average strut leading-edge temperature, 1799° F; average outer-shell lip temperature, 1262° F.

(c) Average plug surface temperature, 1420° F; average strut leading-edge temperature, 1693° F; average outer-shell lip temperature, 1209° F.

Figure 17. - Cooling requirements of air-cooled, conical, variable-area plug nozzle. Average nozzle pressure ratio, 1.95; average nozzle total pressure, 4005 pounds per square foot absolute; average cooling-air temperature, 78° F; average exhaust-gas flow, 101.56 pounds per second. Lip temperatures are for forced-convection film-cooled outer shell.

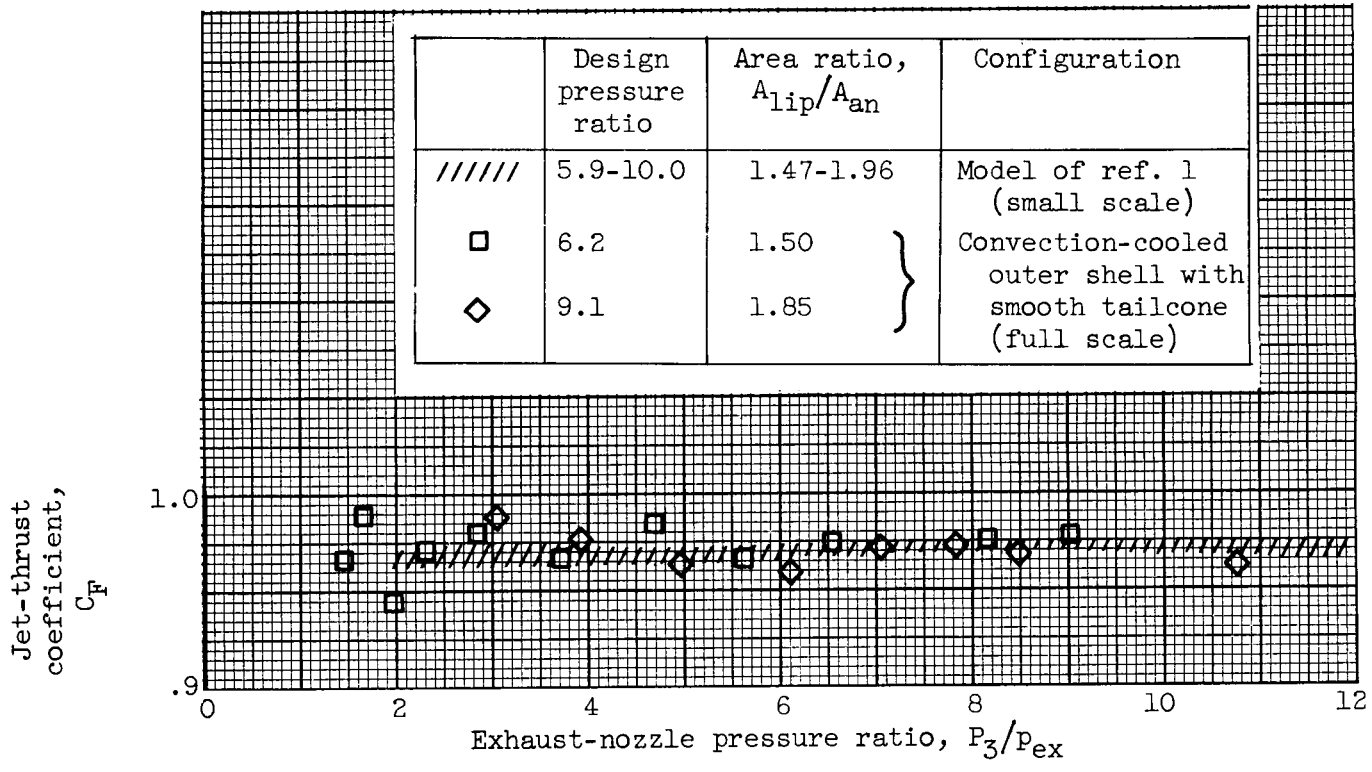

Figure 18. - Effect of nozzle pressure ratio on jet-thrust coefficient with smooth tailcone, no cooling airflow, and no afterburning.

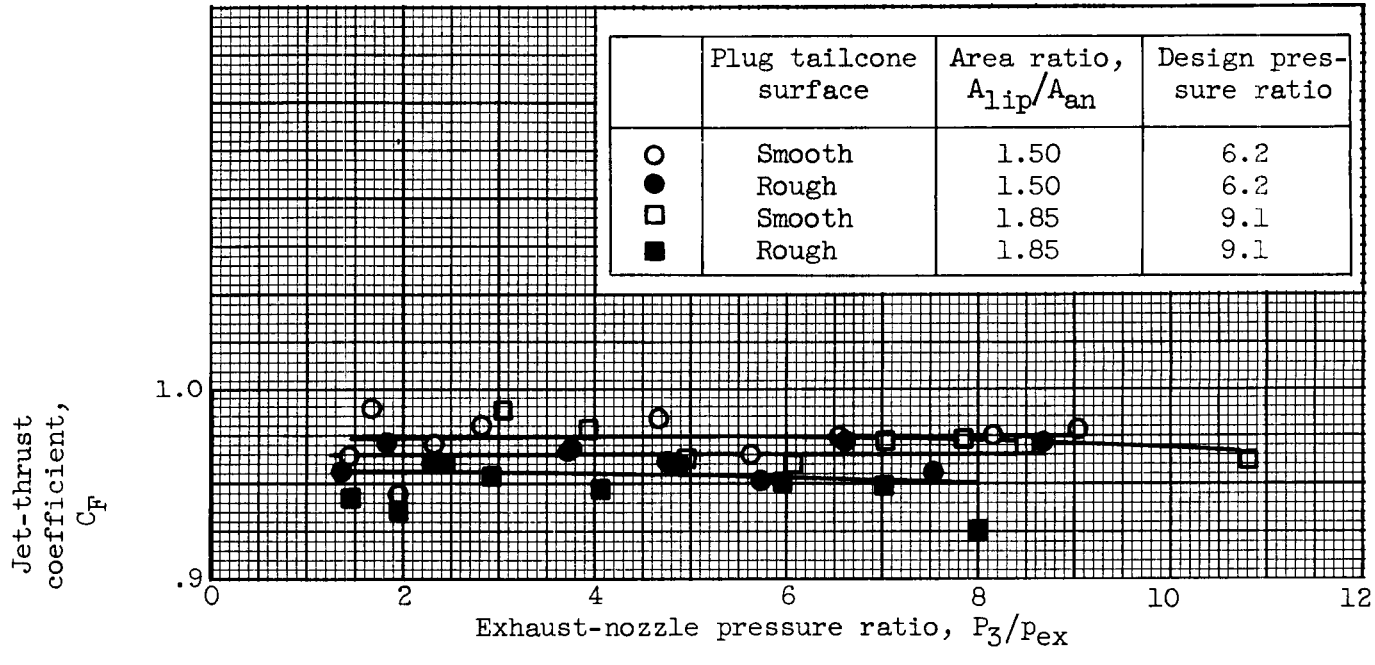

Figure 19. - Effect of plug tailcone roughness on jet-thrust coefficient with a convection-cooled outer shell, no cooling airflow, and no afterburning.

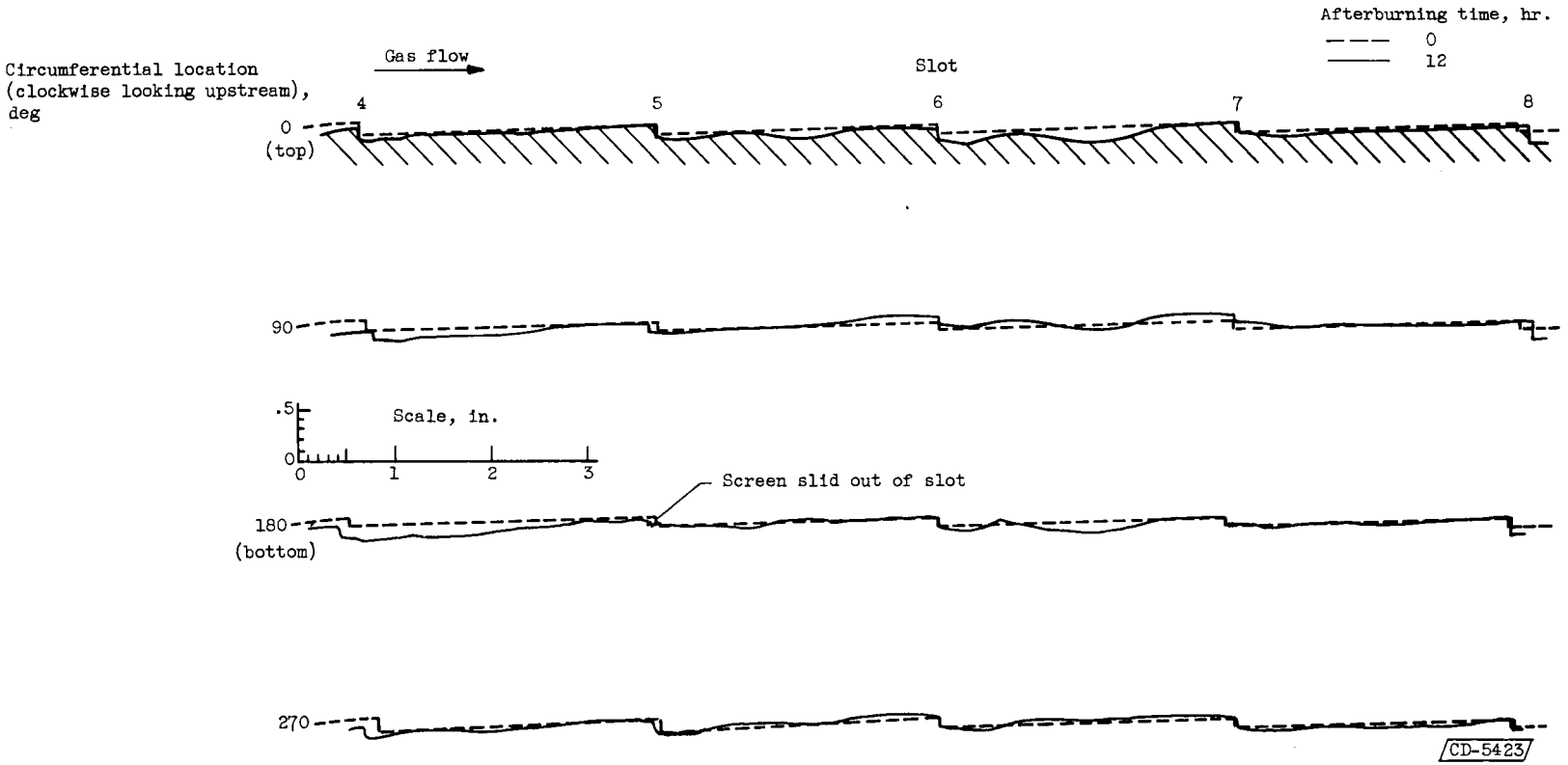

Figure 20. - Plug surface profiles of conical tailcone at beginning and end of afterburning phase.

	Exhaust-nozzle inlet gas flow, $w_{g,3}$, lb/sec	Average exhaust-gas total pressure, P_3, lb/sq ft abs	Average exhaust-gas total temperature, T_3, °F	Average strut cooling-air temperature, °F	Design pressure ratio	Actual pressure ratio, P_3/P_{ex}	Area ratio, A_{lip}/A_{an}
○	83.27	2295	410	61	6.2	6.5	1.50
□	99.31	1946	390	72	3.1	2.7	1.11

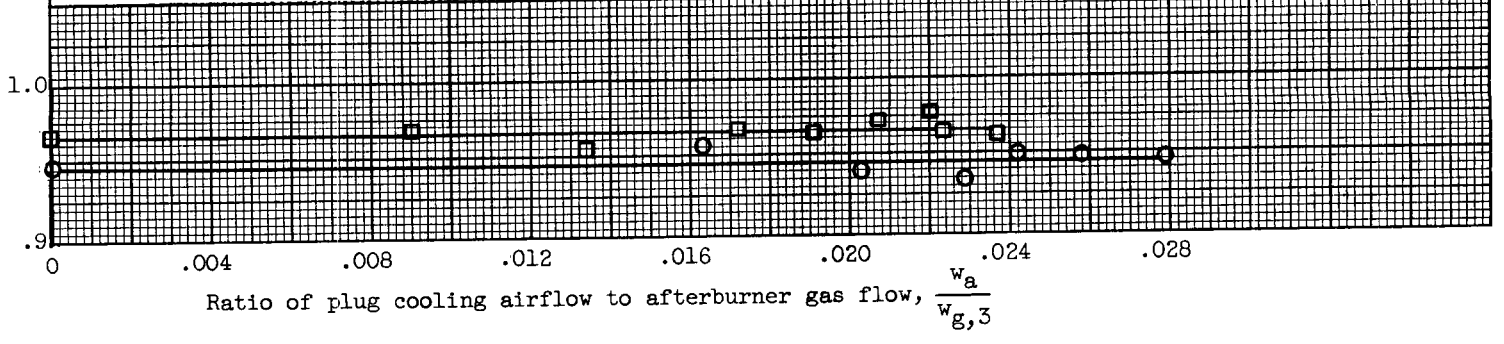

Figure 21. - Effect of plug cooling airflow on jet-thrust coefficient with outer shell cooled with corrugated louvered liner, a rough plug tailcone, and cooling air to plug slots only.

	Exhaust-nozzle inlet gas flow, $w_{g,3}$, lb/sec	Average exhaust-gas pressure, P_3, lb/sq ft abs	Average exhaust-gas total temperature, T_3, ^oF	Average strut cooling-air temperature, ^oF	Design pressure ratio	Actual pressure ratio, P_3/p_{ex}	Area ratio, A_{lip}/A_{an}	Plug tailcone
○	98.69	3272	728	57	9.1	10.8	1.85	Smooth
□	93.74	2988	647	60	9.1	7-10	1.85	Rough

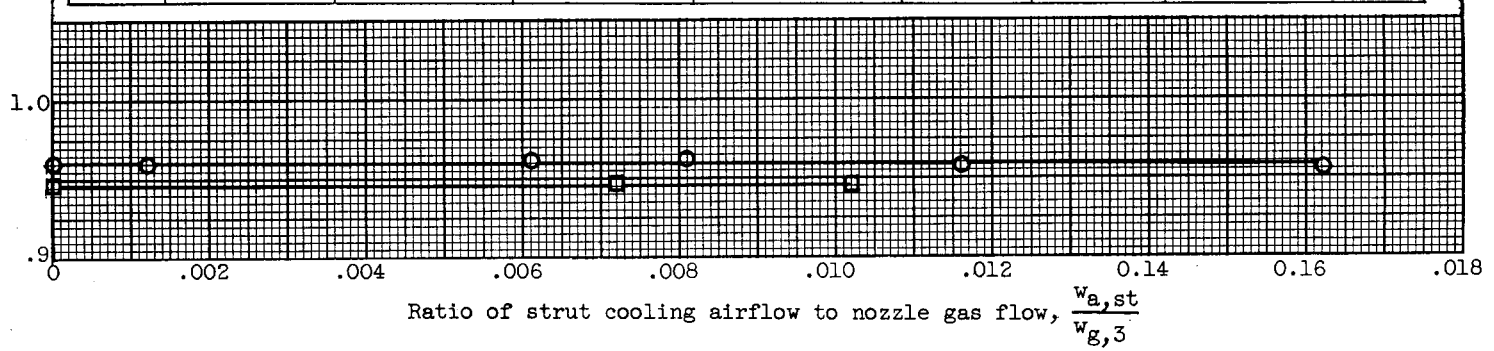

Figure 22. - Effect of strut cooling airflow on jet-thrust coefficient with forced-convection film-cooled outer shell and cooling air to struts only.